CHEMNITZ UNIVERSITY OF TECHNOLOGY

Faculty of Natural Sciences

Computational Physics

Master Thesis

A graphic based interface to Endoreversible Thermodynamics

Katharina Wagner

Chemnitz, July 07, 2008

Tutor: Prof. Dr. Karl Heinz Hoffmann

Wagner, Katharina
A graphic based interface to
Endoreversible Thermodynamics
Master Thesis, Faculty of Natural Sciences
Chemnitz University of Technology, July 2008

Acknowledgment

I want to thank Prof. Hoffmann for his advice and the helpful and interesting discussions. I also want to thank René Haber for the discussions and for providing his assistance with many small problems.

Abstract

The object of this thesis is a graphic based interface to endoreversible thermodynamics. It is meant to enable the user to visually create endoreversible systems and add the properties of the system by choosing features from a list and in form of equations. Then an equation system is built and the power output and efficiency of the endoreversible system is calculated and plotted. To illustrate the functions of the interface, some examples of heat and chemical engines are discussed.

Contents

List of Figures

1 Introduction

Energy transformation processes occurring in reality are always irreversible. In many cases these irreversibilities are important for a realistic description of such processes. Equilibrium thermodynamics, as it evolved during the 19th century, is not capable of considering irreversibilities in an adequate way. It concentrates on reversible processes and systems in equilibrium. In doing so it became a powerful theory but irreversible processes are often approximated as (quasi-static) sequences of equilibria and the irreversibilities are neglected. However, in reality processes are not designed to be reversible or quasi-static, because the desired finite rates for energy transformation require finite and thus irreversible fluxes. Thus the irreversibilities cannot be neglected in a precise description.

One attempt to overcome this classical thermodynamic view has been developed during the last 30 years. It has been labelled endoreversible thermodynamics [19, 20]. In endoreversible thermodynamics a non-equilibrium system is divided into a set of reversible subsystems, which interact with each other by exchanging energy. All the irreversibilities occur in the interactions between the subsystems. Thus for the subsystems itself all the powerful tools and techniques of conventional equilibrium thermodynamics can be used while at the same time dissipative processes are no longer neglected.

In this work an application called 'ETA-Graphics' is presented which enables the user to visually create endoreversible systems by drawing their general structure, i.e. several subsystems connected by interactions. For each interaction the properties, such as energy fluxes, have to be set. Then the application is capable of doing some calculations for the system. The power output and efficiency of engines can be calculated and plotted against each other. It is also possible to change the values of parameters needed for this calculations and thus easily investigate the behaviour of the system under different conditions.

Chapter 2 gives an introduction to the concept of endoreversible thermodynamics in general and the mathematical methods behind it. A first simple example illustrates the use of the theory and its advantages compared to equilibrium thermodynamics.

In chapter 3 the structure of the application and its components is described in detail as well as the way 'ETA-Graphics' is intended to be used.

Some heat engines are then discussed in chapter 4. It mainly focuses on the

Curzon-Ahlborn engine in different variants. A single Curzon-Ahlborn engine as well as one with a heat leak and staged Curzon-Ahlborn engines are considered and their behaviour under different circumstances is investigated both analytically and with the help of 'ETA-Graphics'.

Chapter 5 deals with chemical engines which have a similar structure as the Curzon-Ahlborn heat engine. Nevertheless its structure is not equal and thus there are differences in the general performance of these engines. Single as well as staged chemical engines are considered.

A short conclusion together with an outlook about further improvements of the application is given in chapter 6.

2 Endoreversible thermodynamics

In general an endoreversible system is a network of reversible subsystems that exchange energy. The mathematical description of such an endoreversible system is quite easy. It consists of a set of balance and transport equations forming an equation system. Thus it is similar to electrical networks where the relations between the currents and voltages are defined by the Kirchhoff rules.

However, for endoreversible systems things are a bit more complicated, since energy is not the only quantity that is exchanged. Each energy flux is accompanied by a flux of an extensity, that acts like a carrier for the energy. Such an extensity could, for instance, be the entropy, the angular momentum or the particle number.

A detailed description of endoreversible thermodynamics was published by K. H. Hoffmann et al. in [17] and [15]. In the following I will give an introduction to endoreversible thermodynamics and the mathematical description based on these articles.

2.1 A formal description

The basic building blocks of an endoreversible system are thermal equilibrium subsystems. They are described by their state variables. Because of the equilibrium of the subsystems, one has some freedom in the choice of these state variables. Consider for example an ideal gas. Its state can be described for instance by the volume and the pressure but also by the volume and the entropy. To simplify the theory a special choice of state variables, namely the energy picture, is useful. In this description the energy is considered to be a function of all the other extensive thermodynamic variables of a system.

In the following, X_i^α will denote the extensive thermodynamic variables of subsystem i, like the volume V_i and the particle number N_i, all of which are counted by α. There may be some thermodynamic variables, for example the surface of the subsystem, that are not truly extensive, but for the sake of simplicity here they are called extensive, too. Due to endoreversibility the entropy S_i of subsystem i is a well-defined state variable and belongs to the extensive quantities. Thus the state of the subsystem is uniquely described by the set of its extensities X_i^α and the energy

is

$$E_i = E_i(X_i^\alpha). \tag{2.1}$$

The energy E is not only the internal energy of the subsystem, but it can also include translational kinetic energy, rotational kinetic energy or potential energy in one or more external fields. Elastic energy could also be included. In each case the proper extensive variables have to be included in the set of extensities. Even pure mechanical systems are covered with this description, which is very convenient for instance in the combined treatment of dynamic and thermodynamic systems.

Each extensity has a corresponding intensity. Since the subsystems are in thermodynamic equilibrium, all the standard equilibrium relations hold. Thus the conjugate intensive variables can be obtained from 2.1:

$$Y_i^\alpha = \frac{\partial E_i(X_i^\alpha)}{\partial X_i^\alpha}. \tag{2.2}$$

The conjugate intensive variable for example for the extensity entropy S_i would be the temperature T_i and the corresponding intensity for the angular momentum L_i would be the angular velocity ω_i.

With this definitions the Gibbs equation becomes

$$dE_i = \sum_\alpha Y_i^\alpha dX_i^\alpha. \tag{2.3}$$

Due to the Gibbs equation 2.3 each influx of an extensity $J_i^\alpha = \dot{X}_i^\alpha$ into the system carries an accompanying influx of energy I_i^α with

$$I_i^\alpha = Y_i^\alpha J_i^\alpha. \tag{2.4}$$

For example a heat flux q is carried by an entropy flux q/T and an angular momentum flux M (torque) carries an energy flux ωM, where ω is the angular velocity.

2.1.1 Endoreversible systems

With these definitions it is possible to give a more precise description of endoreversible systems:

Endoreversible systems are networks of reversible subsystems that exchange energy through interactions between them.

Each subsystem i is characterised by a number of contact points through which the subsystem receives or discards energy. Each energy flux is transported by an extensity X_i^α, for example volume or entropy. The contact points for the same extensity in one subsystem are counted by r.

Thus each contact point has three functions assigned to it $(Y_i^{\alpha,r}, J_i^{\alpha,r}, I_i^{\alpha,r})$, where $I_i^{\alpha,r}$ is the flux of energy, $J_i^{\alpha,r}$ is the accompanying flux of the extensity and $Y_i^{\alpha,r}$ is the corresponding thermodynamic intensity for this contact point. Due to endoreversibility these three functions are always related by

$$I_i^{\alpha,r} = Y_i^{\alpha,r} J_i^{\alpha,r}. \tag{2.5}$$

There are two possible types of reversible subsystems, reservoirs and engines, which are described more precisely now.

Reservoirs

A reservoir is a thermodynamic system in equilibrium, which is characterised by either

- given intensities Y_i^α: Reservoirs of this kind are infinite, i.e. the in- or outflux of extensities does not change the value of the intensities Y_i^α. An example would be an infinite heat bath with constant temperature.
- its extensities X_i^α and its energy function $E_i(X_i^\alpha)$: Reservoirs of this kind are finite and their intensities can be determined with the help of the energy function: $Y_i^\alpha = \partial E_i / \partial X_i^\alpha$. Due to its internal equilibrium the intensities are uniform throughout the whole reservoir, i.e. the intensities $Y_i^{\alpha,1} = Y_i^{\alpha,2} = \cdots \equiv Y_i^\alpha$ are equal for all contacts r. From the balance equation for the extensities and the energy one finds

  $$\dot{X}_i^\alpha = \sum_r J_i^{\alpha,r} \tag{2.6}$$

  and

  $$\dot{E}_i = \sum_{\alpha,r} I_i^{\alpha,r} = \sum_{\alpha,r} Y_i^{\alpha,r} J_i^{\alpha,r} = \sum_\alpha Y_i^\alpha \sum_r J_i^{\alpha,r} = \sum_\alpha Y_i^\alpha \dot{X}_i^\alpha. \tag{2.7}$$

  Thus extensities are neither destroyed nor produced within a finite reservoir.

Engines

Engines are reversible subsystems, which transform energy, for example from thermal energy into mechanical energy. Its contact variables are related by special balance re-

quirements for the extensities and the energy, such that neither energy nor extensities are produced or deposited within an engine.

For engines operating in a steady state the balance equations are

$$0 = \sum_r J_i^{\alpha,r} \tag{2.8}$$

for the extensities and

$$0 = \sum_{\alpha,r} I_i^{\alpha,r} = \sum_{\alpha,r} Y_i^{\alpha,r} J_i^{\alpha,r} \tag{2.9}$$

for the energy flux.

For cyclic engines with cycle time t_{tot} the requirements are

$$0 = \int_0^{t_{\mathrm{tot}}} \mathrm{d}t \sum_r J_i^{\alpha,r} \tag{2.10}$$

for the extensity fluxes and

$$0 = \int_0^{t_{\mathrm{tot}}} \mathrm{d}t \sum_{\alpha,r} I_i^{\alpha,r} = \int_0^{t_{\mathrm{tot}}} \mathrm{d}t \sum_{\alpha,r} Y_i^{\alpha,r} J_i^{\alpha,r} \tag{2.11}$$

for the energy flux.

If the cycle time can be divided into branches during which the energy and carrier fluxes remain constant, the integrals can be divided into sums as follows:

$$0 = \sum_b t_b \sum_r J_{i,b}^{\alpha,r} \tag{2.12}$$

for the carrier fluxes and

$$0 = \sum_b t_b \sum_{\alpha,r} I_{i,b}^{\alpha,r} = \sum_b t_b \sum_{\alpha,r} Y_{i,b}^{\alpha,r} J_{i,b}^{\alpha,r} \tag{2.13}$$

for the energy flux.

Interactions

The interactions describe how energy is exchanged between the contact points of two subsystems. The contact points are connected by the interactions in a way such that each contact point belongs to one specific interaction. The interactions

are characterised by the set of contact points they connect and the extensity X_i^α, through which energy is exchanged. There are two kinds of interactions - reversible and irreversible ones. For reversible interactions only the two contact points for the exchanged extensity are needed. In case of irreversible interactions, entropy is produced. Thus at least one additional contact is needed in which the produced entropy can be deposited. The only exception would be an irreversible interaction, for which the carrier is entropy. In this case the produced entropy can be lead through the main interaction and there is no additional contact needed.

Energy and some of the extensities (like angular momentum) are conserved quantities by nature, while others (like the particle number of chemical species) are not. In complete interactions all the conserved quantities must balance to zero.

The two types of interactions are characterised as follows:

- reversible: The intensities at the connected contact points are equal, $Y_i^{\alpha,r} = Y_j^{\alpha,r}$.
- irreversible: The interaction is defined by a transport law which gives either the flux of energy
$$I_i^{\alpha,r} \tag{2.14}$$
or the corresponding flux of an extensity
$$J_i^{\alpha,r} \tag{2.15}$$
at each of the involved contacts. Both, energy and extensity flux, are functions of the intensities, the extensities (for reservoirs) and of additional external parameters. The energy fluxes are different at the two connected contacts and thus the difference specifies the amount of energy that is deposited into the additional contact for irreversible interactions.

2.2 Example: The Novikov engine

Now the formalism of endoreversible thermodynamics described above is applied to a first simple example.

The Novikov engine [18] is, like the Curzon-Ahlborn engine treated later (section 4.1), a system consisting of a reversible, continuously working Carnot engine [3], which is connected with two infinite heat reservoirs. The internal temperatures of this Carnot engine are T_{iH} and T_{iL}, with $T_{\mathrm{iH}} > T_{\mathrm{iL}}$. The Carnot engine is in direct contact with the heat bath of the lower temperature T_{L}. Thus the lower temperature

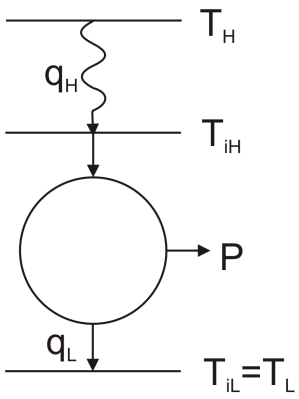

Figure 2.1: The Novikov engine consisting of a reversible Carnot-like engine, which is coupled irreversibly with the high temperature heat bath T_{H}. The connection with the low temperature heat bath T_{L} is reversible.

at the Carnot engine equals the temperature of the external heat bath, $T_{\mathrm{iL}} = T_{\mathrm{L}}$. The coupling to the external bath of higher temperature T_{H} is irreversible and is characterised by a finite heat conductance K. Figure 2.1 shows the structure of the Novikov engine. The two external heat baths are considered to be infinite and thus an in- or outflux of energy does not change their temperatures.

In the picture of endoreversible systems the Novikov engine consists of one engine - the Carnot engine - and a couple of reservoirs. Both heat baths are infinite reservoirs characterised by an intensity, namely their temperature. The Carnot engine transforms a part of the thermal energy received from the high temperature bath into mechanical energy. Let us assume that a shaft is driven with constant angular velocity ω_{D}. Then there are two more reservoirs needed – one that absorbs the energy transmitted by the angular momentum of the shaft (subsystem 4, see figure 2.2) and another one to fix the engine such that the shaft rotates and not the engine itself (subsystem 3). For the sake of simplicity both of these reservoirs are considered to be infinite and in direct contact with the engine. The interaction between the engine and the latter of the two reservoirs is characterised by an angular velocity $\omega_{\mathrm{C}} = 0$.

The interactions between these subsystems are characterised as follows: For the direct contact between the engine and the low temperature heat bath the extensity is the entropy S and thus the corresponding intensity is the temperature T_{L}. The flux of energy (or heat flux) q_{L} is not limited by the reservoir but by the balance equations of the engine (as we will see later). The flux of entropy accompanying the heat flux is $q_{\mathrm{L}}/T_{\mathrm{L}}$. Since the interaction is reversible this is all that is needed to fully describe it.

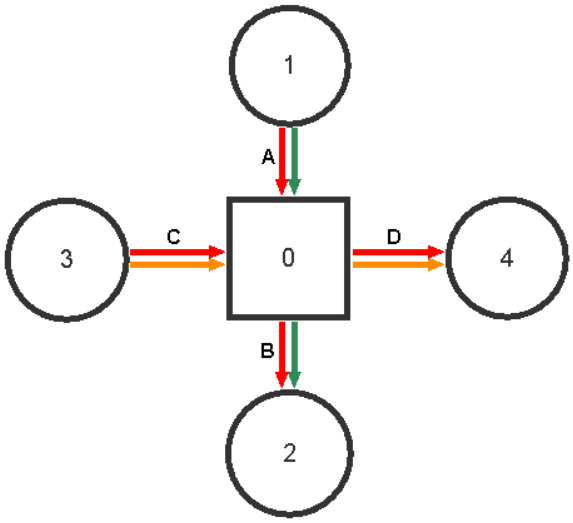

Figure 2.2: The Novikov engine in 'ETA-Graphics'. Subsystem 0 represents the engine, subsystems 1 and 2 are the high and low temperature heat baths and subsystems 3 and 4 are angular momentum reservoirs.

The interaction between the engine and reservoir 3 is defined by the extensity L_C (angular momentum) and the intensity ω_C (angular velocity). Since $\omega_C = 0$, the energy flux $I_C = \omega_C M_C$, where M_C is the angular momentum flux (torque), equals zero. However, the angular momentum flux M_C does not equal zero.

The interaction between the engine and reservoir 4 is characterised by the angular momentum L_D and the angular velocity ω_D. Thus the energy flux is $I_D = \omega_D M_D$, where M_D is the flux of angular momentum. The energy flux I_D represents the mechanical power output of the Novikov engine and thus a quantity of interest in further calculations.

Between the high temperature heat bath and the engine there is an irreversible interaction. The energy flux is defined by a transport law for heat. Let us assume Newtonian heat conduction, i.e. the energy flux is $q_H = K(T_H - T_{iH})$, where K is a constant heat conductance. Since entropy is the extensity of this interaction, the produced entropy due to irreversibility can be absorbed by the contact at the engine and there is no additional reservoir needed in this case. Thus the entropy flux at the contact at the engine is $K(T_H - T_{iH})/T_{iH}$, while at the contact point at the reservoir the entropy flux is $K(T_H - T_{iH})/T_H$, which is bigger since $T_H > T_{iH}$.

With these subsystems and interactions the Novikov engine is fully described and the balance equations for the Carnot engine can be set up.

The balance equation for the energy flux (equ. 2.9) gives

$$0 = q_{\mathrm{H}} - q_{\mathrm{L}} - \omega_{\mathrm{D}} M_{\mathrm{D}} = K(T_{\mathrm{H}} - T_{\mathrm{iH}}) - q_{\mathrm{L}} - \omega_{\mathrm{D}} M_{\mathrm{D}} \tag{2.16}$$

and from the balance equations for the extensity fluxes (equ. 2.8) one gets

$$0 = M_{\mathrm{C}} - M_{\mathrm{D}} \quad \text{and} \tag{2.17}$$

$$0 = \frac{q_{\mathrm{H}}}{T_{\mathrm{iH}}} - \frac{q_{\mathrm{L}}}{T_{\mathrm{L}}} = \frac{K(T_{\mathrm{H}} - T_{\mathrm{iH}})}{T_{\mathrm{iH}}} - \frac{q_{\mathrm{L}}}{T_{\mathrm{L}}}. \tag{2.18}$$

Solving the equation system containing equations (2.16), (2.17) and (2.18) one obtains:

$$q_{\mathrm{L}} = \frac{T_{\mathrm{L}}}{T_{\mathrm{iH}}} K(T_{\mathrm{H}} - T_{\mathrm{iH}}) \tag{2.19}$$

$$M_{\mathrm{D}} = M_{\mathrm{C}} \tag{2.20}$$

$$\omega_{\mathrm{D}} = \frac{K(T_{\mathrm{H}} - T_{\mathrm{iH}})(1 - \frac{T_{\mathrm{L}}}{T_{\mathrm{iH}}})}{M_{\mathrm{C}}}. \tag{2.21}$$

Thus the engine's power output P becomes

$$P = \omega_{\mathrm{D}} M_{\mathrm{D}} = K(T_{\mathrm{H}} - T_{\mathrm{iH}})(1 - \frac{T_{\mathrm{L}}}{T_{\mathrm{iH}}}). \tag{2.22}$$

The maximum power is determined by setting the derivative of P with respect to T_{iH} equal to zero:

$$0 = \frac{\mathrm{d}P}{\mathrm{d}T_{\mathrm{iH}}} = K\left(\frac{T_{\mathrm{H}} T_{\mathrm{L}}}{T_{\mathrm{iH}}^2} - 1\right), \tag{2.23}$$

from which we obtain $T_{\mathrm{iH}} = \sqrt{T_{\mathrm{H}} T_{\mathrm{L}}}$. Inserting this temperature into equation 2.22 gives the maximum power output,

$$P_{\max} = K(\sqrt{T_{\mathrm{H}}} - \sqrt{T_{\mathrm{L}}})^2. \tag{2.24}$$

Using equation 2.19 the efficiency for a Novikov engine can be written as

$$\eta = \frac{q_{\mathrm{H}} - q_{\mathrm{L}}}{q_{\mathrm{H}}} = 1 - \frac{q_{\mathrm{L}}}{q_{\mathrm{H}}} = 1 - \frac{T_{\mathrm{L}}}{T_{\mathrm{iH}}}. \tag{2.25}$$

Thus the efficiency at maximum power, i.e. with $T_{\mathrm{iH}} = \sqrt{T_{\mathrm{H}} T_{\mathrm{L}}}$, is

$$\eta(P_{\max}) = 1 - \frac{T_{\mathrm{L}}}{\sqrt{T_{\mathrm{H}} T_{\mathrm{L}}}} = 1 - \sqrt{\frac{T_{\mathrm{L}}}{T_{\mathrm{H}}}}. \tag{2.26}$$

Note that the efficiency at the point of maximum power output does not depend on the heat conductance K but only on the bath temperatures T_{H} and T_{L}.

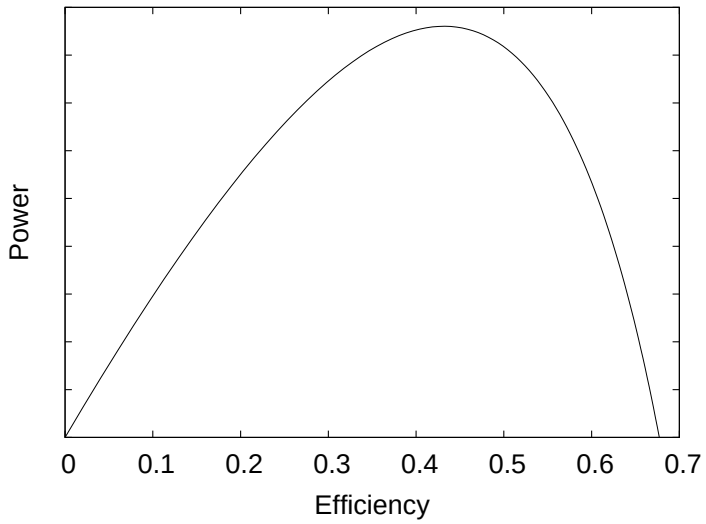

Figure 2.3: Power vs. efficiency for a Novikov engine working between the temperatures $T_{\mathrm{H}} = 650°\mathrm{C}$ and $T_{\mathrm{L}} = 25°\mathrm{C}$. The maximum efficiency is $\eta_{\max} = 1 - T_{\mathrm{L}}/T_{\mathrm{H}} = 0.68$ and the efficiency at maximum power is $\eta(P_{\max}) = 1 - \sqrt{T_{\mathrm{L}}/T_{\mathrm{H}}} = 0.43$.

A plot of the power over the efficiency for a Novikov engine can be seen in figure 2.3. The ratio between the temperatures of the external reservoirs for this curve is $T_{\mathrm{L}}/T_{\mathrm{H}} = 0.32$. Thus the efficiency at maximum power output is $\eta(P_{\max}) = 0.43$.

Since the efficiency depends linearly on the inverse temperature T_{iH}^{-1}, the maximum efficiency cannot be calculated by setting the derivative with respect to T_{iH} equal to zero. But from the power-efficiency curve one can see, that the maximum efficiency for a Novikov engine can be obtained by solving the equation $P = 0$ for T_{iH}:

$$0 = K(T_{\mathrm{H}} - T_{\mathrm{iH}})(1 - \frac{T_{\mathrm{L}}}{T_{\mathrm{iH}}}) \rightarrow T_{\mathrm{iH}}^{(1)} = T_{\mathrm{H}}, \quad T_{\mathrm{iH}}^{(2)} = T_{\mathrm{L}}. \tag{2.27}$$

For $T_{\mathrm{iH}}^{(2)}$ the efficiency equals zero. Therefore the maximum efficiency is at $T_{\mathrm{iH}}^{(1)}$:

$$\eta_{\max} = 1 - \frac{T_{\mathrm{L}}}{T_{\mathrm{H}}}. \tag{2.28}$$

Thus the maximum efficiency equals the Carnot efficiency, which is quite reasonable, since the Novikov engine becomes a simple Carnot engine when $T_{\mathrm{iH}} = T_{\mathrm{H}}$.

3 ETA-Graphics

The aim of this graphic based interface to endoreversible thermodynamics is to enable users to visually construct an endoreversible system by drawing subsystems (reservoirs and engines) and connecting them with interactions. By specifying the interactions, i.e. by choosing the extensity and its corresponding intensity and inserting the energy and carrier flux, the (thermodynamic) properties of the system are set.

The application is called 'ETA-Graphics', where ETA stands for 'Endoreversible Thermodynamics Application' and also referrs to the Greek letter η, which is used as a symbol for the efficiency. This seems suitable, since the efficiency is calculated by 'ETA-Graphics'.

3.1 Software requirements

Since the interface is developed in Java, one needs the Java Runtime Environment (JRE) version 5.0 update 14 or a newer version to run 'ETA-Graphics'. The JRE is available for free at java.com. A second requirement is Wolfram Mathematica [22] to perform the calculations. The application is developed and tested with version 6.0.0 but it may run with older versions as well. Without Mathematica the endoreversible systems can still be created but the calculations cannot be performed.

3.2 Components of the interface

3.2.1 Main window

The main window contains different areas. The drawing panel is the area where the endoreversible system is constructed by the user. At the beginning it is a plain white area. To draw a new subsystem the 'Add Subsystem' button has to be selected. Then a new subsystem can be drawn by pressing the left mouse button and dragging the occurring circle to the wanted size. As the mouse button is released, the 'New system' dialogue appears (see fig. 3.1), where the system type, i.e. reservoir or engine, has

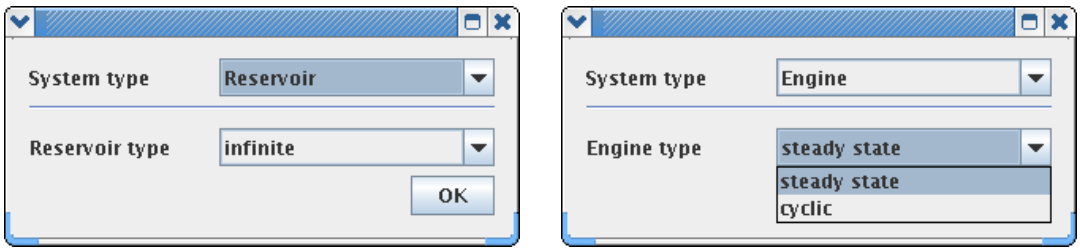

Figure 3.1: The dialogue for a new subsystem in 'ETA-Graphics'. In this dialogue the user has to choose, whether the new subsystem is a reservoir (left screenshot) or an engine (right screenshot). If engine is chosen, the type has to be selected as well, i.e. whether it is a steady state engine or a cyclic engine.

to be selected. For engines it is then possible to set whether it is a steady state or a cyclic operating engine. If 'Engine' is selected as system type the shape of the subsystem changes from a circle to a square. Thus engines and reservoirs can be easily distinguished. All subsystems are labelled with an index that is shown at their centre.

Interactions are added by choosing the 'Add Interaction' button and then clicking on the subsystem, from which energy is transported to another subsystem. As the first subsystem is selected two parallel arrows representing the interaction occur and a second system, where the energy is transported to, can be selected by clicking into another subsystem. As soon as both subsystems are chosen a dialogue appears, where the properties of the interaction can be set (see section 3.2.2). The third subsystem, where the produced entropy for irreversible interactions is deposited to, is added after setting the properties of the interaction. But it is only added in case of irreversibility.
The interactions are labelled with letters, which are shown next to the arrows. Each interaction is represented by two parallel arrows illustrating both, the flux of energy and the flux of the corresponding extensity. The energy arrow is red and the second arrow's color is defined by the extensity that is transported through this interaction. If the interaction is irreversible, it splits up into two arrows - one for the entropy produced due to irreversibility and one for the carrier chosen in the properties dialogue (see for example interaction A in fig. 3.2).

The intensities get an index according to the system and the interaction they belong to, i.e. the first index is the number of the system and the second index is the letter of the interaction. If the interaction is reversible the intensities at both of the connected systems are equal. Therefore they only get the index of the interaction

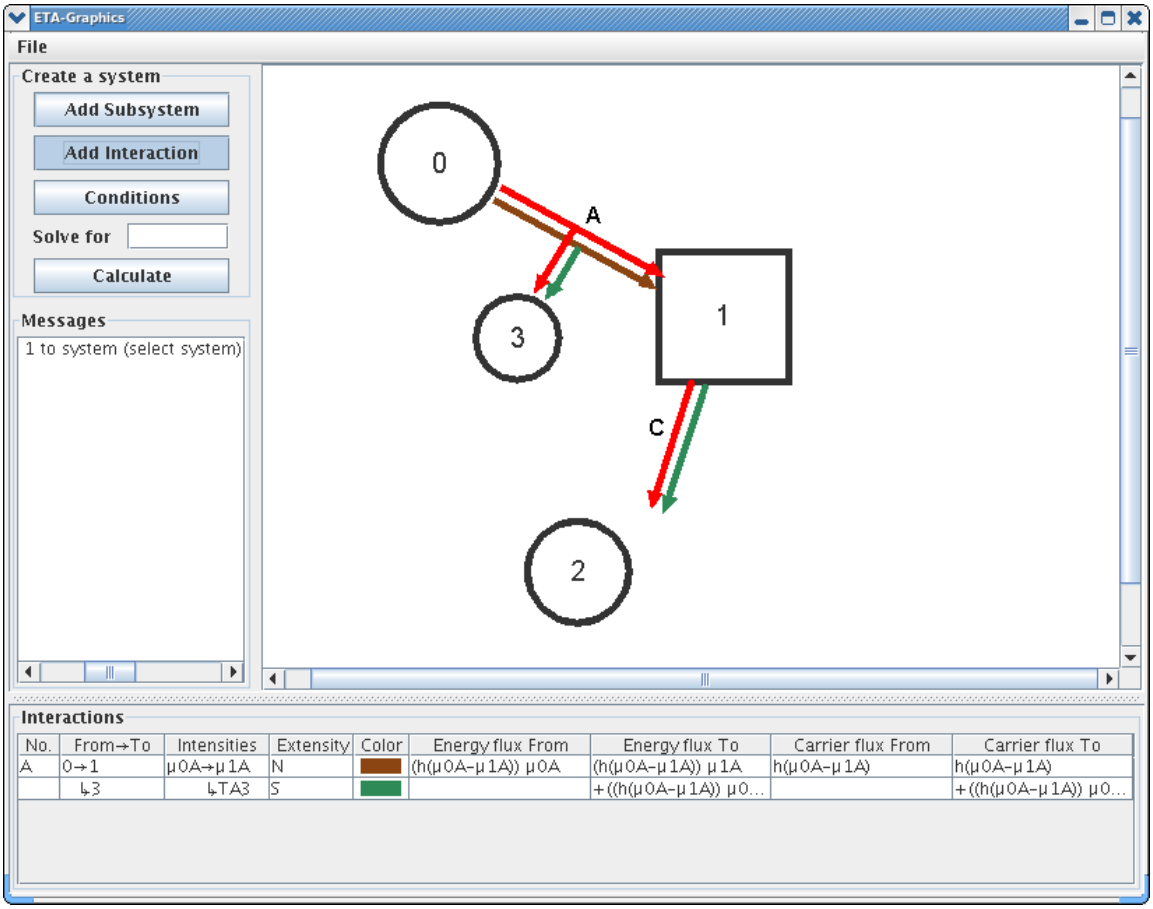

Figure 3.2: Main window of 'ETA-Graphics'. In the upper left corner the buttons needed for drawing the subsystems and interactions can be seen. In the upper right corner there is the drawing area. The interaction table is situated at the bottom of the main window.

they belong to.

Other elements of the main window are a table, where all the interactions and its properties are listed, and the buttons needed for creating a system and the calculations.

3.2.2 Interaction properties dialogue

With the help of the interaction properties dialogue (see fig. 3.3) the extensity of the interaction is chosen from a list. The corresponding intensity is added automatically.

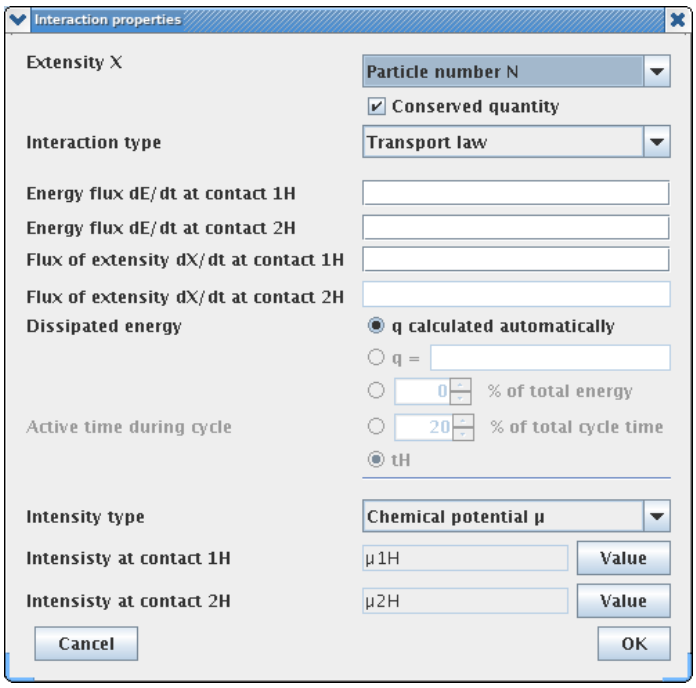

Figure 3.3: The interaction properties dialogue of 'ETA-Graphics'. In this dialogue the extensity and the intensity of the interaction and the interaction type, i.e. direct contact or transport law, are chosen. If the interaction is irreversible, the energy and extensity fluxes have to be set. If the system is cyclic, determination of the cycle time is needed, too.

(It is also possible to select the intensity first and then the corresponding extensity is automatically set.) Below the extensity there is a check box that gives the user the possibility to choose whether the extensity is conserved at this interaction. In addition it is possible (but not necessary) to assign values to the intensities at the two connected subsystems. The buttons to do this are right next to the intensities.

If the user wants to choose an extensity that is not listed, there is the possibility to select 'Add another extensity' from the drop down list. Then a dialogue appears where a new extensity as well as the corresponding intensity and symbols for both of them have to be entered. There is also a check box where the user decides whether the new quantity should be included in the power output needed for the efficiency calculation. The user can also choose the color, in which the arrows for this extensity should be painted. The new extensity-intensity-set is stored in the file 'extensities.xml' so that it need not be added again.

The next field gives the opportunity to choose whether the interaction should be

reversible (selection 'Direct contact') or irreversible (selection 'Transport law'). In the reversible case the two subsystems are in direct contact without external limitations with regard to the energy and carrier flux. However, internal balance requirements can limit the amount of energy transported.
In case of irreversibility the interaction is defined by a transport law either for the exchanged energy or the extensity that carries the energy. In the dialogue there are four fields, in which transport laws for the energy or the carrier at the two connected subsystems respectively can be inserted. If 'Conserved quantity' is selected, the carrier fluxes at the connected systems have to be equal. Thus only one of the fields for carrier fluxes is enabled and the second one is filled automatically.
If the energy flux at one contact point is set, the corresponding extensity flux is added automatically and vice versa. That is possible because energy and extensity flux are connected by equation 2.5.

For irreversible interactions a third subsystem is added to the interaction. It is a reservoir, where the produced entropy or the dissipated energy is deposited to. If the extensity is a conserved quantity, the amount of dissipated energy is calculated automatically from the difference between the energy fluxes at the two connected subsystems. If the extensity is not a conserved quantity, there are three possibilities to set the amount of dissipated energy. As soon as both energy fluxes are set, the dissipated energy is calculated automatically. The second way is to specify only one energy flux and the percentage of the total energy that is transported to the extra reservoir. For example one can set that 5 per cent of the total energy is transformed into heat due to dissipation processes. The third possibility is to give an equation for the dissipated energy and one energy flux.

If the extensity for an irreversible interaction is entropy, it is possible to deposit the additionally produced entropy via the main interaction and there is no third contact needed.

3.2.3 Interaction table

In the interaction table at the bottom of the main window (see figure 3.2), all interactions of the system are listed. In the first column one can find the labels of the interaction. The second column shows which subsystems are connected by this interaction. The extensity, through which energy is transported, and the colour, in which its arrow is drawn, are also listed (column 4 and 5) as well as the corresponding intensities at the connected contact points (column 3). The last four columns contain the fluxes of energy and of the extensity at the two main contacts of the interaction.

If an interaction is irreversible the part of the interaction for the dissipated energy is also listed in the table in an extra row. Since it is not a single interaction that

connects two subsystems, all the cells, which represent quantities at the subsystem where the interaction starts, remain empty. In column 2 only the subsystem, which takes the produced entropy, is listed.

If the interaction is reversible, the fluxes of energy and an extensity are equal at both ends of the interaction. Thus they are only printed once in the interaction table and the field for the fluxes at the beginning of the interaction are empty.

The interaction table is also the place where interactions can be edited or deleted. By selecting an interaction and then right-clicking, a menu with the options 'Delete Interaction' and 'Edit Interaction' is opened. When 'Edit Interaction' is chosen, the same dialogue as for a new interaction appears but the fields are already filled with the current properties of the interaction. Then these properties can be changed. If 'Delete Interaction' is chosen from the menu, the selected interaction is removed. If the removed interaction was irreversible, the reservoir for the dissipated energy is removed as well if it has no other interactions. It is not possible to edit or delete the row, which contains the part of an interaction for entropy deposition, on its own. These rows can only be changed via the main interaction they belong to.

3.2.4 Solution window

By pushing the 'Calculate' button an equation system is created. For each engine in the system the balance equations - one for the energy flux and one for each extensity flowing in and out of the engine - are formed (see section 2.1.1). All these equations are put into one equation system, which is then solved by Mathematica [22]. The variables, for which the system should be solved, can be entered in the 'Solve for' field above the 'Calculate' button. If this field is left blank, the application chooses the variables by itself, observing the following rules:

1. The number of variables chosen equals the number of balance equations.

2. First of all the variables occurring in the equation for the power output of the engines are chosen, i.e. from those interactions, whose extensities are chosen to be considered for the power output. These variables are chosen first because the power output is the quantity of interest in most cases. For the Novikov engine this would be ω_{D} and M_{D}.

3. Then, if needed, the variables from the other output (e.g. heat) are considered following a hierarchy according to their position. That means variables at engines are chosen before those at reservoirs and before external parameters. For the Novikov engine this gives q_{L}.

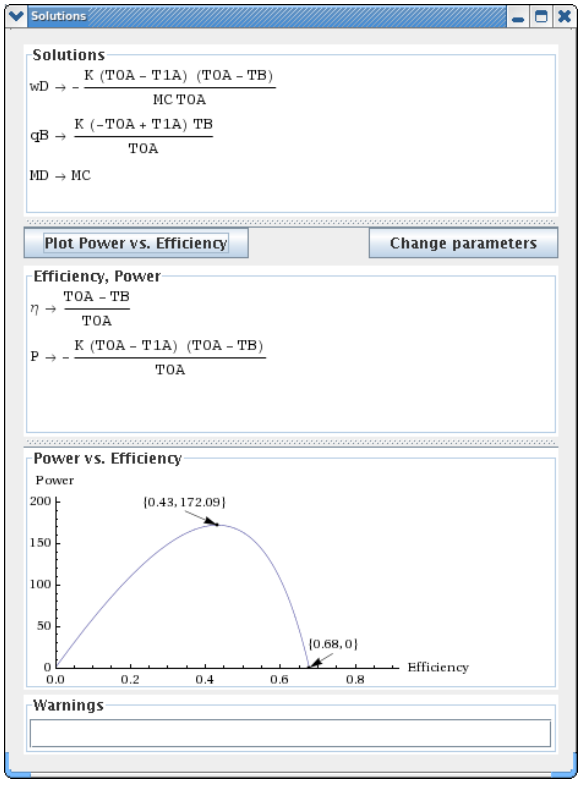

Figure 3.4: The solution window of 'ETA-Graphics'. The solutions of the equation system can be seen at the top of the window. In the middle the efficiency and the power output of the system are displayed and at the bottom of the window the power vs. efficiency plot is shown.

4. If there are still variables needed afterwards, i.e. the number of balance equations is still bigger than the number of variables, then the variables from the input equations are considered. For the Novikov engine there are no more variables needed, since there are only three balance equations (one for the energy, one for entropy, and one for angular momentum) and there are two variables from the power output equation and on from the heat output.

The solutions for the equation system, which are calculated using Mathematica, are then shown in a new window (see fig. 3.4). This window also contains some more components. It is possible to calculate the efficiency and the power output of an endoreversible engine and plot these two quantities against each other. In order to get this plot some additional input is needed. Therefore after pressing the 'Plot Power vs. Efficiency'-button the user is asked to assign values to the variables occurring in the equations for efficiency and power (see fig. 3.5). One variable has to be chosen as

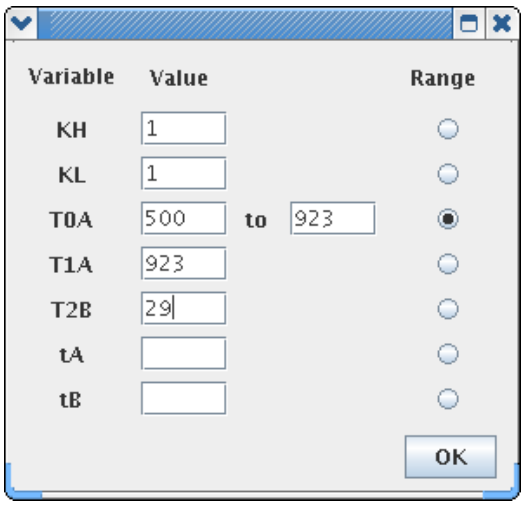

Figure 3.5: The dialogue for the input of values for the variables occurring in the efficiency and power equation. One of the variables has to be chosen as the parameter for the plot and a range for this parameter has to be set. For all other variables the input of a value is needed.

the parameter, which changes within a user-specified range to produce a parametric plot of the power versus the efficiency. The equations for the power output and the efficiency are both shown in the solution window beneath the solution of the equation systems.

There is another button, which can be used to change the input made for the plot. After pressing the 'Change parameters'-button the same window as for the initial input occurs but the current values are shown. Thus they can be changed and it is easy to get the plot for different combinations of values.

3.3 Menu structure

3.3.1 File menu

Load and save

It is possible to save an endoreversible system created in 'ETA-Graphics'. By selecting the 'Save' menu item the current system is stored as an XML-file. All the subsystems and its interactions as well as the properties of the interactions are saved.

With the ‘Load’ menu item these files can be loaded into ‘ETA-Graphics’. The system is drawn to the drawing panel and the interaction properties are written in the interactions table. Then this system can be edited and calculations can be made.

Properties

In the properties dialogue some settings needed for Mathematica have to be made. If the application is running on Windows or Mac OS X the directory, where the MathKernel can be found, has to be set. On Unix this is not necessary.

The properties dialogue is shown automatically when the application is started for the first time. Then the settings are saved since normally there is no need to change them again. Only if the directory of the MathKernel changes (e.g. after installing a newer version) the settings have to be updated via the menu item ‘Properties’.

Reset

The reset menu item can be used to delete the current system completely. The drawing panel is cleared as well as the interactions table. The application is set back to its initial configuration which it has after the start of ‘ETA-Graphics’. The image files produced during the calculations are also deleted.

All of this is also done when a new system is loaded from an XML-file and when the user quits the application.

Quit

When the ‘Quit’ menu item is chosen, the reset is run to delete the image files produced in background and the application is exited.

4 Heat engines

In this chapter some more complex heat engines are investigated with the help of 'ETA-Graphics' to show how it works and what results can be achieved using it. The focus lies on different types of Novikov and Curzon-Ahlborn engines. Different heat transfer laws (sec. 4.4) are considered as well as heat leaks (sec. 4.2 and 4.3.2) and combinations of two heat engines (sec. 4.3).

4.1 The Curzon-Ahlborn engine

The Curzon-Ahlborn engine [9] is a heat engine that transforms heat into mechanical power. It consists of a cyclic Carnot engine operating between the higher temperature T_{iH} and the lower temperature T_{iL}. The Carnot engine is coupled with two heat reservoirs at the constant temperatures T_{H} and T_{L} and the coupling is irreversible and obeys the Newtonian heat transfer law. Figure 4.1 shows the schematic structure of a Curzon-Ahlborn engine. Part of the thermal energy influx is transformed into mechanical energy. In this example it is assumed that a shaft is driven with angular velocity ω. For the sake of simplicity the mechanical interactions are considered to be reversible, i.e. there is for instance no loss of energy through friction. Thus the finite-rate heat transfers between the heat reservoirs and the engine are the only irreversibilities occurring in this system.

4.1.1 Analytical approach

Curzon-Ahlborn engines have been widely discussed in literature. The maximum power output as well as the optimal efficiency and optimal operation paths have been investigated (see, for instance, [13, 16, 19, 20]).

The heat transferred between the high temperature reservoir and the engine is given by

$$Q_{\mathrm{H}} = K_{\mathrm{H}} t_{\mathrm{H}} (T_{\mathrm{H}} - T_{\mathrm{iH}}) \tag{4.1}$$

and the heat transferred between the engine and the low temperature reservoir is given by

$$Q_{\mathrm{L}} = K_{\mathrm{L}} t_{\mathrm{L}} (T_{\mathrm{iL}} - T_{\mathrm{L}}). \tag{4.2}$$

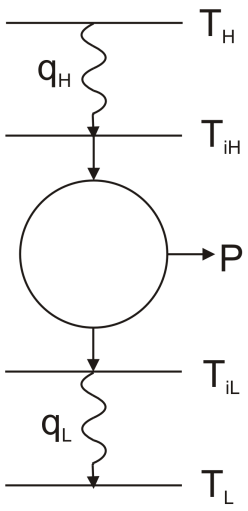

Figure 4.1: The Curzon-Ahlborn engine consisting of a reversible engine in the centre with the working temperatures T_{iH} and T_{iL} and two infinite heat baths with temperatures T_{H} and T_{L}. The couplings between the engine and the two reservoirs are irreversible.

The total cycle time for the engine is denoted with t_{tot}. The time spent in the isentropic branches of the cycle is considered to be negligible. Thus the total cycle time can be divided into t_{H} and t_{L}; $t_{\mathrm{tot}} = t_{\mathrm{H}} + t_{\mathrm{L}}$. t_{H} is the time during which the heat from the high temperature reservoir is transported to the engine while during the time t_{L} heat is transferred to the low temperature reservoir.

According to equation 2.11 the energy fluxes of the Carnot engine subsystem balance during a whole cycle:

$$0 = Q_{\mathrm{H}} - Q_{\mathrm{L}} - W, \tag{4.3}$$

where W is the work performed by the engine.

The balance equation for the carrier (see equation 2.10), i.e. the entropy, can be written as

$$0 = \Delta S_{\mathrm{H}} - \Delta S_{\mathrm{L}} = \frac{Q_{\mathrm{H}}}{T_{\mathrm{iH}}} - \frac{Q_{\mathrm{L}}}{T_{\mathrm{iL}}}. \tag{4.4}$$

Combining equations 4.3 and 4.4 one obtains

$$W = Q_{\mathrm{H}} - Q_{\mathrm{L}} = Q_{\mathrm{H}}(1 - \frac{T_{\mathrm{iL}}}{T_{\mathrm{iH}}}) = Q_{\mathrm{H}}(1 - \tau), \tag{4.5}$$

where τ is defined as $T_{\mathrm{iL}}/T_{\mathrm{iH}}$.

With 4.1, 4.2 and 4.4 τ can be written as

$$\tau = \frac{Q_\mathrm{L}}{Q_\mathrm{H}} = \frac{K_\mathrm{L} t_\mathrm{L}(T_\mathrm{iL} - T_\mathrm{L})}{K_\mathrm{H} t_\mathrm{H}(T_\mathrm{H} - T_\mathrm{iH})} = \frac{K_\mathrm{L} t_\mathrm{L}(\tau T_\mathrm{iH} - T_\mathrm{L})}{K_\mathrm{H} t_\mathrm{H}(T_\mathrm{H} - T_\mathrm{iH})}. \tag{4.6}$$

Solving 4.6 for T_iH and inserting into 4.5 yields

$$W = (1-\tau)(T_\mathrm{H} - \frac{T_\mathrm{L}}{\tau})\frac{K_\mathrm{H} K_\mathrm{L} t_\mathrm{H} t_\mathrm{L}}{K_\mathrm{H} t_\mathrm{H} + K_\mathrm{L} t_\mathrm{L}} = C T_\mathrm{H} \eta \frac{\eta_\mathrm{C} - \eta}{1 - \eta} \tag{4.7}$$

with the efficiencies

$$\eta_\mathrm{C} = 1 - \frac{T_\mathrm{L}}{T_\mathrm{H}} \quad \text{and} \tag{4.8}$$

$$\eta = 1 - \frac{T_\mathrm{iL}}{T_\mathrm{iH}} = 1 - \tau \tag{4.9}$$

and

$$C = \left(\frac{1}{K_\mathrm{H} t_\mathrm{H}} + \frac{1}{K_\mathrm{L} t_\mathrm{L}}\right)^{-1} = \left(\frac{1}{K_\mathrm{H} t_\mathrm{H}} + \frac{1}{K_\mathrm{L}(t_\mathrm{tot} - t_\mathrm{H})}\right)^{-1}. \tag{4.10}$$

Now the maximum power output per cycle can be obtained by setting both $(\partial W/\partial \eta)_{t_\mathrm{H}}$ and $(\partial W/\partial t_\mathrm{H})_\eta$ to zero. Since C depends only on t_H and not on η the problem factorises nicely.

The condition $(\partial W/\partial \eta)_{t_\mathrm{H}} = 0$ gives a relation between the branch times and the heat conductance coefficients:

$$\frac{t_\mathrm{H}}{t_\mathrm{L}} = \frac{\sqrt{K_\mathrm{L}}}{\sqrt{K_\mathrm{H}}}. \tag{4.11}$$

The second condition, $(\partial W/\partial t_\mathrm{H})_\eta = 0$, leads to the Curzon-Ahlborn efficiency

$$\eta(W_\mathrm{max}) = \eta_\mathrm{CA} = 1 - \sqrt{T_\mathrm{L}/T_\mathrm{H}} \tag{4.12}$$

at maximum work. The maximum work can be obtained by inserting 4.11 and 4.12 into 4.7:

$$W_\mathrm{max} = t_\mathrm{tot} \frac{K_\mathrm{H} K_\mathrm{L}}{\left(\sqrt{K_\mathrm{H}} + \sqrt{K_\mathrm{L}}\right)^2} \left(\sqrt{T_\mathrm{H}} - \sqrt{T_\mathrm{L}}\right)^2. \tag{4.13}$$

Comparisons with real power plants showed that the Curzon-Ahlborn efficiency is much more realistic than the Carnot efficiency η_C. Tables with comparisons can for instance be found in a paper by Curzon and Ahlborn [9] or in the book 'Advanced Engineering Thermodynamics' by Bejan [2].

The maximum efficiency can be obtained by setting $W(\eta)$ (equation 4.7) equal to zero:

$$\eta_\mathrm{max} = \eta_\mathrm{C} = 1 - \frac{T_\mathrm{L}}{T_\mathrm{H}}. \tag{4.14}$$

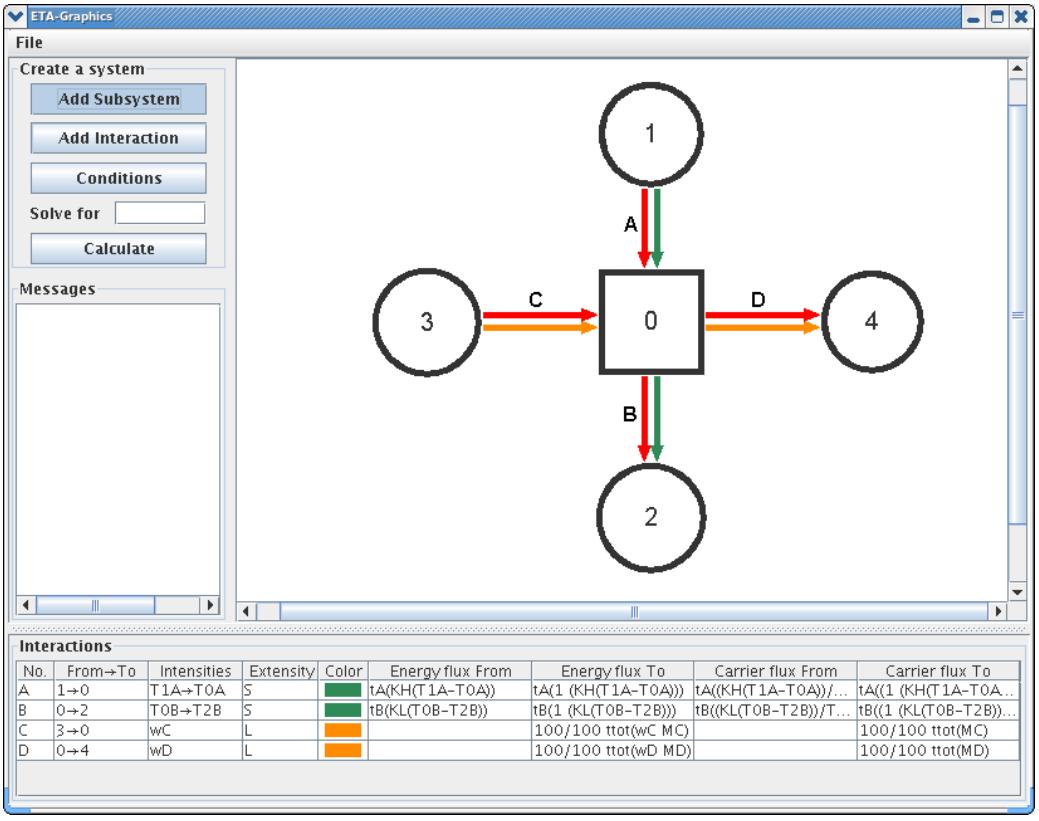

Figure 4.2: The Curzon-Ahlborn engine in 'ETA-Graphics'. Subsystem 0 represents the engine, subsystems 1 and 2 are the heat baths, and subsystems 3 and 4 are reservoirs for mechanical quantities.

4.1.2 The Curzon-Ahlborn engine in 'ETA-Graphics'

Figure 4.2 shows a screenshot of the engine's structure in 'ETA-Graphics'. The square in the centre represents the Carnot engine and the circles with number 1 and 2 are the two infinite heat reservoirs. In addition there are two reservoirs needed: One (system 4) that takes the mechanical energy outflux of the Carnot engine and one (system 3) to fix the engine. This fixation is needed because otherwise the engine and the shaft would rotate antipodal. Since the angular velocity at the reservoir representing the fixation is zero, the engine gets no energy influx through this interaction. There is also a mathematical explanation for the need of system 3. Since the fluxes of extensities within the engine balance to zero (see equation 2.10), the angular momentum flux from the engine to system 4 would be zero (and thus the energy flux) if there was no additional system 3.

The four interactions of the system are characterised as follows:
For the interactions A and B the extensity is the entropy S and thus the corresponding intensity is the temperature T. Both of these interactions are irreversible but since their extensity is entropy the additionally produced entropy can be lead through the Carnot engine and there is no additional system needed to deposit it. The heat that is absorbed by the engine through interaction A is

$$Q_{\mathrm{A}} = K_{\mathrm{H}} t_{\mathrm{H}} (T_{1\mathrm{A}} - T_{0\mathrm{A}}) \tag{4.15}$$

with $T_{1\mathrm{A}} \equiv T_{\mathrm{H}}$ and $T_{0\mathrm{A}} \equiv T_{\mathrm{iH}}$. The corresponding carrying extensity at the Carnot engine is

$$S_{0\mathrm{A}} = \frac{K_{\mathrm{H}} t_{\mathrm{H}} (T_{1\mathrm{A}} - T_{0\mathrm{A}})}{T_{0\mathrm{A}}}. \tag{4.16}$$

For interaction B the heat leaving the engine is set to

$$Q_{\mathrm{B}} = K_{\mathrm{L}} t_{\mathrm{L}} (T_{0\mathrm{B}} - T_{2\mathrm{B}}) \tag{4.17}$$

with $T_{0\mathrm{B}} \equiv T_{\mathrm{iL}}$ and $T_{2\mathrm{B}} \equiv T_{\mathrm{L}}$. The corresponding extensity flux at the Carnot engine is

$$S_{0\mathrm{B}} = \frac{K_{\mathrm{L}} t_{\mathrm{L}} (T_{0\mathrm{B}} - T_{2\mathrm{B}})}{T_{0\mathrm{B}}}. \tag{4.18}$$

The interactions C and D are both assumed to be reversible.
The energy flux at interaction C equals zero because the angular velocity ω_{C} is zero (mechanical fixation of the engine). However, the flux of the extensity, i.e. the angular momentum flux $\dot{L}_{\mathrm{C}} = M_{\mathrm{C}}$, is not zero.
For interaction D the energy flux is defined as the product of angular velocity and torque, $\omega_{\mathrm{D}} M_{\mathrm{D}}$. Thus the corresponding flux of the extensity is M_{D}.

With these properties the Curzon-Ahlborn engine is fully characterised. By pushing the 'Calculate' button the equation system containing the system's three balance equations for energy, entropy and angular momentum flux is solved for ω_{D}, M_{D} and $T_{0\mathrm{B}}$. One gets:

$$\omega_{\mathrm{D}} = \frac{K_{\mathrm{H}} t_{\mathrm{H}} (T_{1\mathrm{A}} - T_{0\mathrm{A}} + \frac{K_{\mathrm{L}} (T_{0\mathrm{A}} - T_{1\mathrm{A}}) T_{2\mathrm{B}} t_{\mathrm{L}}}{K_{\mathrm{H}} (T_{0\mathrm{A}} - T_{1\mathrm{A}}) t_{\mathrm{H}} + K_{\mathrm{L}} T_{0\mathrm{A}} t_{\mathrm{L}}})}{M_{\mathrm{C}} t_{\mathrm{tot}}} \tag{4.19}$$

$$M_{\mathrm{D}} = M_{\mathrm{C}} \tag{4.20}$$

$$T_{0\mathrm{B}} = \frac{K_{\mathrm{L}} T_{0\mathrm{A}} T_{2\mathrm{B}} t_{\mathrm{L}}}{K_{\mathrm{H}} (T_{0\mathrm{A}} - T_{1\mathrm{A}}) t_{\mathrm{H}} + K_{\mathrm{L}} T_{0\mathrm{A}} t_{\mathrm{L}}}. \tag{4.21}$$

Now the power output and the efficiency of the engine can be calculated and plotted against each other by pressing the 'Plot Power vs. Efficiency' button. The resulting equations for the power output and the efficiency calculated by 'ETA-Graphics'

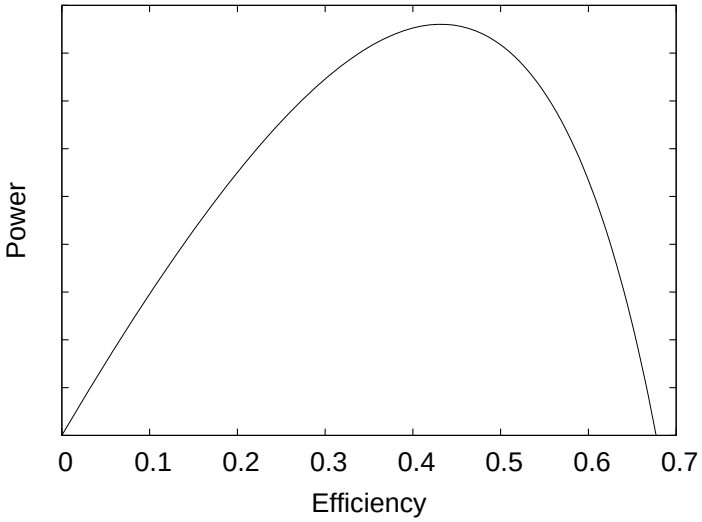

Figure 4.3: Power vs. efficiency curve for the Curzon-Ahlborn engine working between the temperatures $T_{\mathrm{H}} = 650°\mathrm{C}$ and $T_{\mathrm{L}} = 25°\mathrm{C}$. The efficiency at the point of maximum power is $\eta(P_{\max}) = 1 - \sqrt{T_{\mathrm{L}}/T_{\mathrm{H}}} = 0.43$ and the maximum efficiency is the Carnot efficiency, $\eta_{\max} = \eta_{\mathrm{C}} = 1 - T_{\mathrm{L}}/T_{\mathrm{H}} = 0.68$.

are

$$P = K_{\mathrm{H}} \left(T_{1\mathrm{A}} - T_{0\mathrm{A}} - \frac{K_{\mathrm{L}} T_{2\mathrm{B}} (T_{1\mathrm{A}} - T_{0\mathrm{A}})}{K_{\mathrm{L}} T_{0\mathrm{A}} - K_{\mathrm{H}} (T_{1\mathrm{A}} - T_{0\mathrm{A}})} \right) \quad \text{and} \tag{4.22}$$

$$\eta = \frac{K_{\mathrm{L}} (T_{0\mathrm{A}} - T_{2\mathrm{B}}) - K_{\mathrm{H}} (T_{1\mathrm{A}} - T_{0\mathrm{A}})}{K_{\mathrm{L}} T_{0\mathrm{A}} - K_{\mathrm{H}} (T_{1\mathrm{A}} - T_{0\mathrm{A}})}. \tag{4.23}$$

Then the user has to decide which of the variables in the power and efficiency equation should be the parameter for the plot. This parameter is then changed within an user-specified range in order to get the plot. The user is also asked to give values for the constants and parameters in the power and efficiency equation.

The resulting plot can be seen in figure 4.3. The temperature $T_{0\mathrm{A}}$ was chosen as the parameter for this plot. The ratio $T_{\mathrm{L}}/T_{\mathrm{H}}$ is 0.32 and thus the power maximum is reached at the efficiency $\eta(P_{\max}) = 1 - \sqrt{T_{\mathrm{L}}/T_{\mathrm{H}}} = 0.43$ and the maximum efficiency is $\eta_{\max} = \eta_{\mathrm{C}} = 1 - T_{\mathrm{L}}/T_{\mathrm{H}} = 0.68$, which is the Carnot efficiency.

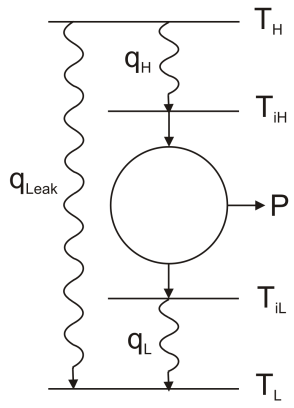

Figure 4.4: The structure of a Curzon-Ahlborn engine with heat leak. The leak is included as an irreversible interaction between the external heat reservoirs. The heat leak has no influence on the power output of the engine but on the efficiency.

4.2 Heat engines with heat leaks

In real heat engines it is not avoidable to loose some of the heat via heat leaks. For example through the walls of combustion chambers and engines heat is lost. These losses significantly influence the performance of the engines and therefore should not be neglected.

In figure 4.4 the structure of an extended Curzon-Ahlborn engine with a heat leak is shown. Part of the heat coming out of the high temperature reservoir is going directly to the low temperature reservoir.

This heat leak has neither an influence on the balance equations nor on the work output of the engine. However, it affects the efficiency of the engine since the heat lost through the leak is included in the work or energy input that is needed to calculate the efficiency. Thus the efficiency is given as

$$\eta = \frac{W_{\text{out}}}{Q_{\text{in}} + Q_{\text{leak}}}. \tag{4.24}$$

Let us assume the heat transfer law for the heat leak as well as for the two other irreversible heat transfers is the Newtonian heat transfer law, i.e. the amount of heat is proportional to the temperature difference ($Q_{\text{leak}} = K_{\text{leak}} t_{\text{tot}} (T_{\text{H}} - T_{\text{L}})$).

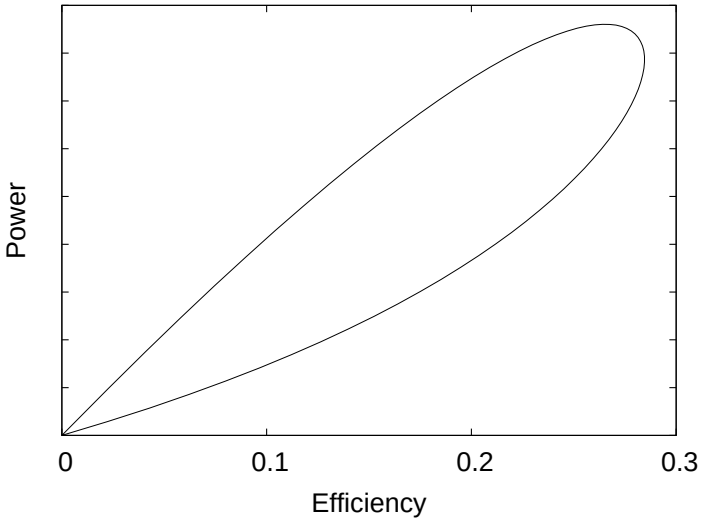

Figure 4.5: Power vs. efficiency plot for the Curzon-Ahlborn engine with heat leak working between the temperatures $T_\mathrm{H} = 650°\mathrm{C}$ and $T_\mathrm{L} = 25°\mathrm{C}$. The heat conductances are $K_\mathrm{H} = K_\mathrm{L} = 1$ and $K_\mathrm{leak} = 0.1$.

Thus the the efficiency becomes

$$\eta = \frac{P}{Q_\mathrm{H} + K_\mathrm{leak} t_\mathrm{tot} (T_\mathrm{H} - T_\mathrm{L})}. \tag{4.25}$$

Figure 4.5 shows a plot of the average power (work per cycle time) P versus the efficiency η. The plot shows the loop-type behaviour for engines with heat leaks, which is remarkably different from the behaviour of engines without heat leak. The operation points of maximum power and maximum efficiency are close together, but the efficiency maximum is much smaller than the Carnot efficiency.

If the temperature T_iH is high, i.e. close to T_H, Q_H is small and thus the power output is very small, too. Since the heat lost through the heat leak remains constant, the efficiency approaches zero. The second case where the efficiency vanishes is when the temperature T_iH gets smaller and thus equal to T_iL. In this case the power output of the engine approaches zero (cf. power-efficiency plot of a Curzon-Ahlborn engine without heat leak; fig. 4.3). Since again the heat lost through the heat leak remains constant, the efficiency approaches zero.

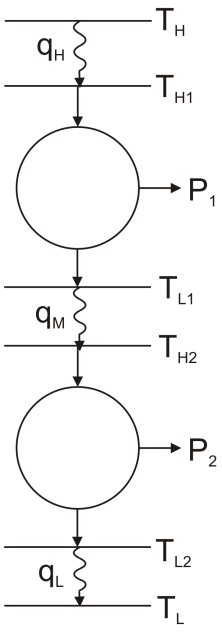

Figure 4.6: A two-staged Curzon-Ahlborn engine working between the temperatures T_{H} and T_{L}. The waste heat of the upper engine is totally used as the heat source of the lower engine. The couplings between the two engines and between the reservoirs and the engines are irreversible.

4.3 Staged heat engines

In the chapters before only single Carnot-like engines were considered. However, in many applications several energy transformation devices are coupled. For example in power plants the waste energy of a high temperature cycle is often used as the heat source of a low temperature cycle. In this chapter the combination of two endoreversible engines will be investigated with the help of 'ETA-Graphics'.

Two Curzon-Ahlborn engines are combined in a way, such that the waste heat from the first engine is totally used as the heat source of the second engine. The engines are operating between a high temperature reservoir T_{H} and a low temperature reservoir T_{L} (see figure 4.6).

Rubin and Andresen discussed this kind of staged heat engine in great detail [21] and found that for a Curzon-Ahlborn engine operating between the temperatures T_{H} and T_{L} the efficiency at maximum total power output does not change if the single engine is replaced by two Curzon-Ahlborn engines.

Chen and Wu [6, 5] also investigated systems of two and more combined Curzon-Ahlborn engines and calculated the efficiency as well as the total power output.
In [5] Chen also investigated staged Curzon-Ahlborn engines with heat leaks, which show the same qualitative behaviour as single Curzon-Ahlborn engines with a heat leak.

4.3.1 A two-staged Curzon-Ahlborn engine in 'ETA-Graphics'

Figure 4.7 shows a staged heat engine consisting of two Curzon-Ahlborn engines. The interactions C, G, and H are characterised by a Newtonian heat transfer law of the form

$$q_i = K_i(T_{i\mathrm{H}} - T_{i\mathrm{L}}), \tag{4.26}$$

where $T_{i\mathrm{H}}$ is the higher temperature at the beginning of the arrow and $T_{i\mathrm{L}}$ is the lower temperature at the end of the arrow. K_i is the heat conductance coefficient for the interaction i. Interactions A, B, E, and F are direct contacts, for which angular momentum is the extensity and angular velocity the corresponding intensity. At interactions A and E the angular velocities equal zero, $\omega_\mathrm{A} = \omega_\mathrm{E} = 0$, since these interactions represent the fixation of the engines.

A plot of the power over the efficiency for a two-staged Curzon-Ahlborn engine can be seen in figure 4.8. It has the same shape as for a single Curzon-Ahlborn engine with the only difference that the maximum power output for the two-staged engine is 2/3 of the power output of a single engine if the heat conductances K_i are equal. That can easily be understood. The thermal resistance of a single Curzon-Ahlborn engine is $1/K_\mathrm{H} + 1/K_\mathrm{L}$, which becomes $2/K$ if $K_\mathrm{H} = K_\mathrm{L} = K$. For the staged engine the thermal resistance is $1/K_\mathrm{H} + 1/K_\mathrm{M} + 1/K_\mathrm{L} = 3/K$ (for $K_\mathrm{H} = K_\mathrm{M} = K_\mathrm{L} = K$). Thus the thermal resistance of the staged Curzon-Ahlborn engine is 1.5 times higher than that of single engine, which leads to 2/3 of the power output [21].

4.3.2 A two-staged Curzon-Ahlborn engine with heat leak

Now a heat leak is added to the staged Curzon-Ahlborn engine investigated before. In 'ETA-Graphics' it is included as an irreversible interaction between the high and the low temperature reservoirs. The energy flux for this interaction is

$$q_\mathrm{leak} = K_\mathrm{leak}(T_\mathrm{H} - T_\mathrm{L}). \tag{4.27}$$

In figure 4.9 the influence of the heat conductance K_leak on the shape of the power-efficiency plot is shown. The shape of the curve converges to the shape of the power-efficiency curve of the engine without heat leak the smaller K_leak becomes.

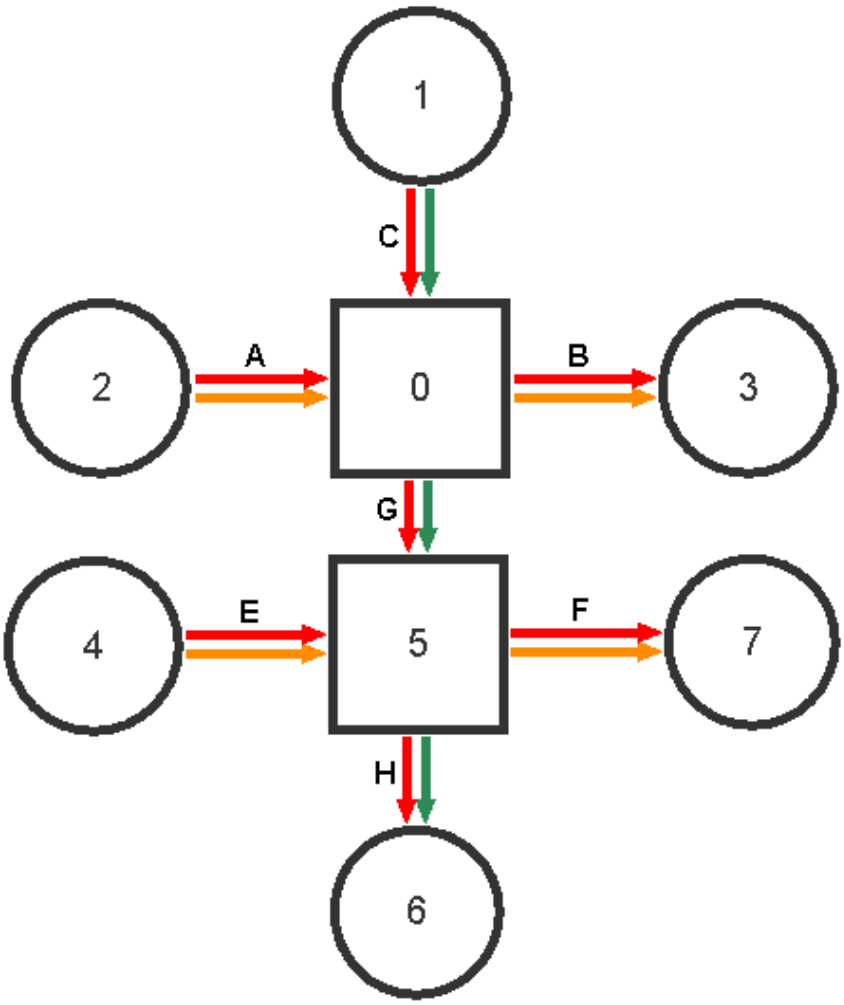

Figure 4.7: A two-staged Curzon-Ahlborn engine in 'ETA-Graphics'. Subsystems 1 and 6 are the heat reservoirs, subsystems 0 and 5 are the two engines and subsystems 2 to 4 and 7 are angular velocity reservoirs. The interactions C, G, and H are irreversible and the interactions A, B, E, and F are reversible.

4.4 Heat transfer laws

So far only the Newtonian heat transfer law has been considered both for the Novikov and the Curzon-Ahlborn engine. Other heat transfer laws are possible as well and in general they are more complicated than the Newtonian heat transfer law. The form of the transfer law significantly influences the behaviour of endoreversible systems.

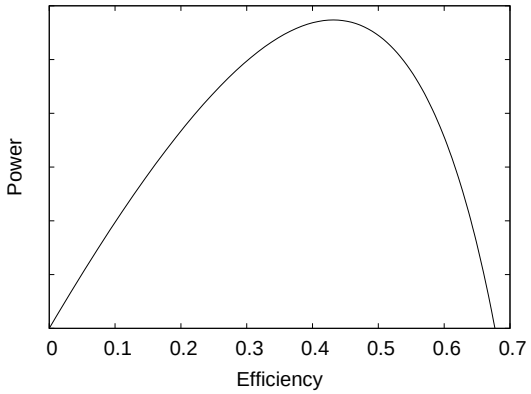

Figure 4.8: Power-efficiency plot for a two-staged Curzon-Ahlborn engine. The point of maximum power output lies at the efficiency $\eta(P_{\max}) = 1 - \sqrt{(T_{\mathrm{L}}/T_{\mathrm{H}})} = 0.43$ and the maximum efficiency is $\eta_{\max} = 1 - T_{\mathrm{L}}/T_{\mathrm{H}} = 0.68$.

This can be seen in the power vs. efficiency curve (fig. 4.10).

In the following an overview over some heat transfer laws, that are used in literature in general and for Novikov and Curzon-Ahlborn engines in particular, is given. All of them have in common that the energy flow depends on the temperatures of the two contacts connected.

4.4.1 Newtonian heat transfer law

The Newtonian heat conduction has already been used in section 2.2 and 4.1. It is a linear heat transfer law that assumes the heat flow to be proportional to the temperature differences of the two connected contacts:

$$q = K(T_1 - T_2). \tag{4.28}$$

Because of its simplicity this heat transfer law has been widely used to study the performance of endoreversible systems [5, 6, 9, 21]. It is a good approximation for heat fluxes in solids. But it can also be applied to other heat transfer mechanisms like convection if the temperature differences are small, since a dominating linear term frequently occurs in the Taylor expansion of more general, non-linear transfer laws.

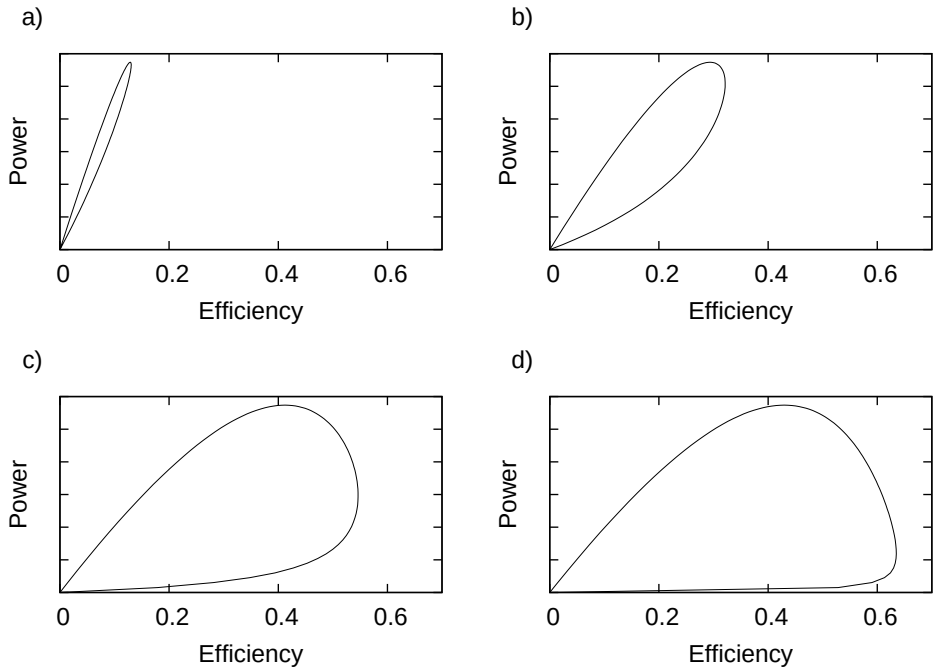

Figure 4.9: Power-efficiency plot for a two-staged Curzon-Ahlborn engine with heat leak. To show the dependency on the heat conductance of the heat leak, K_{leak} is set to a) $K_{\text{leak}} = 0.5$, b) $K_{\text{leak}} = 0.1$, c) $K_{\text{leak}} = 0.01$, and d) $K_{\text{leak}} = 0.001$.

4.4.2 Radiation

Electromagnetic radiation from a hot body like the sun can serve as a heat source for an endoreversible engine. For systems operating at high temperatures radiation is the major transfer mechanism for heat. Typically it is described by the Stefan-Boltzmann law for black-body radiation. Then the heat flux between two radiating bodies at temperatures T_1 and T_2 is given by

$$q = K_1 T_1^4 - K_2 T_2^4, \tag{4.29}$$

where the coefficients K depend on the Stefan-Boltzmann constant, the emittances of the two radiating bodies, and geometry factors.

This heat transfer law is typical for solar collectors.

Example: Novikov engine with radiation

For a Novikov engine with radiation instead of a Newtonian heat transfer law the balance equations are slightly different. The equation for the heat flux between the high temperature bath and the engine is

$$q_{\mathrm{H}} = K_{\mathrm{H}} T_{\mathrm{H}}^4 - K_{\mathrm{iH}} T_{\mathrm{iH}}^4, \tag{4.30}$$

while the heat flux between the engine and the low temperature heat bath remains q_{L}, like in section 2.2.

Thus the balance equation for the energy fluxes is

$$P = q_{\mathrm{H}} - q_{\mathrm{L}} = K_{\mathrm{H}} T_{\mathrm{H}}^4 - K_{\mathrm{iH}} T_{\mathrm{iH}}^4 - q_{\mathrm{L}} \tag{4.31}$$

and the balance equation for the entropy gives

$$\frac{K_{\mathrm{H}} T_{\mathrm{H}}^4 - K_{\mathrm{iH}} T_{\mathrm{iH}}^4}{T_{\mathrm{iH}}} = \frac{q_{\mathrm{L}}}{T_{\mathrm{L}}}. \tag{4.32}$$

From equations 4.31 and 4.32 follows

$$P = (K_{\mathrm{H}} T_{\mathrm{H}}^4 - K_{\mathrm{iH}} T_{\mathrm{iH}}^4) \left(1 - \frac{T_{\mathrm{L}}}{T_{\mathrm{iH}}}\right). \tag{4.33}$$

The efficiency can easily be obtained from equation 4.33:

$$\eta = \frac{P}{q_{\mathrm{H}}} = 1 - \frac{T_{\mathrm{L}}}{T_{\mathrm{iH}}}. \tag{4.34}$$

The efficiency is linearly dependent on T_{iH}^{-1} in a way such that the maximum efficiency is reached for the highest possible temperature $T_{\mathrm{iH}}^{\mathrm{max}}$. Since T_{iH} cannot be higher than the temperature of the high temperature heat bath, we get: $T_{\mathrm{iH}}^{\mathrm{max}} = T_{\mathrm{H}}$ and thus again the maximum efficiency equals the Carnot efficiency:

$$\eta_{\mathrm{max}} = \eta_{\mathrm{CA}} = 1 - \frac{T_{\mathrm{L}}}{T_{\mathrm{H}}}. \tag{4.35}$$

Using equations 4.34 and 4.33, the power as a function of η can be obtained:

$$P(\eta) = \left(K_{\mathrm{H}} T_{\mathrm{H}}^4 - K_{\mathrm{iH}} \left(\frac{T_{\mathrm{L}}}{1-\eta}\right)^4\right) \eta. \tag{4.36}$$

A plot of the power over the efficiency for a Novikov engine with radiation can be seen in figure 4.10. One can see that the point of maximum power for a Novikov engine with radiation lies at a higher efficiency than the one for a Novikov engine with Newtonian heat transfer.

4.4.3 Fourier heat transfer law

The Fourier heat transfer law assumes that the heat flow is proportional to the difference of the inverse temperatures,

$$q = K\left(\frac{1}{T_2} - \frac{1}{T_1}\right), \tag{4.37}$$

where K is an Onsager coefficient.

The power-efficiency plot for a Novikov engine with a Fourier heat transfer law between the high temperature reservoir and the engine can be seen in figure 4.10. The efficiency at maximum power is $\eta(P_{\max}) = 0.5(1 - T_{\mathrm{L}}/T_{\mathrm{H}})$.

4.4.4 Dulong-Petit

In some cases the heat transfer is a combination of different laws mentioned before. For example conductive as well as radiative components can occur together and neither of them can be ignored. The so-called Dulong-Petit law,

$$q = K(T_1 - T_2)^n, \tag{4.38}$$

is an attempt to describe a combined conductive-convective and radiative heat transfer in a simplified fashion. K is a proportionality constant and the exponent n is usually in the range between 1.1 and 1.6 [10]. Angulo-Brown and Páez-Hernández [1] obtained good results using the Dulong-Petit law with $n = 5/4$ for investigating the Curzon-Ahlborn model. They predicted theoretical efficiencies for power plants that were very close to the observed efficiencies.

The power-efficiency plot for a Novikov engine with a Dulong-Petit heat transfer law between the high temperature reservoir and the engine can be seen in figure 4.10. For this curve the parameter n is set to 1.25.

4.4.5 Generalised heat transfer law

A generalised heat transfer law is of the form

$$q = K_1 T_1^n - K_2 T_2^m \tag{4.39}$$

which includes the Newtonian ($n = m = 1$ and $K_1 = K_2 = K$), the Fourier ($n = m = -1$ and $K_1 = K_2 = K$), and the radiative ($n = m = 4$) heat transfer law as special cases.

Generalised heat transfer laws have been investigated e.g. by Gordon [12].

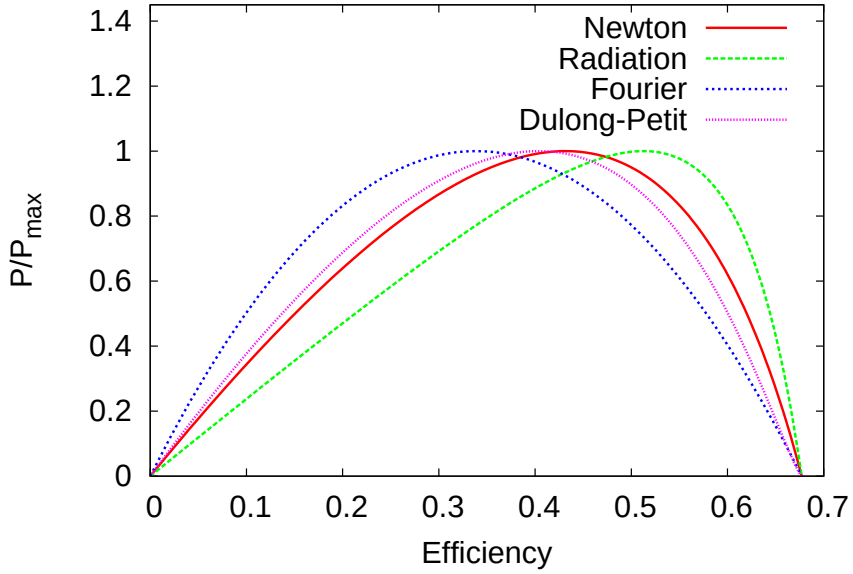

Figure 4.10: Power vs. efficiency for a Novikov engine with different heat transfer laws. The temperatures of the external heat baths are the same. Thus the maximum efficiency is $\eta_{\max} = 0.68$. For better comparability the power is normalised, so that the maximum power is 1. The efficiencies at maximum power are: 0.43 for Newtonian heat transfer, 0.51 for radiation, 0.34 for Fourier heat transfer, and 0.4 for Dulong-Petit heat transfer with $n = 1.25$.

4.4.6 A Novikov engine with different heat transfer laws

Figure 4.10 shows the power-efficiency plot for a Novikov engine with different heat transfer laws characterising the interaction between the high temperature heat bath and the engine. For better comparability $P/P_{\max}$ instead of P is plotted. It can be seen, that the shapes of the curves are slightly different. For example the point of maximum power output is reached at different efficiencies while the maximum efficiency remains the Carnot efficiency.

The same plot was made for a Novikov engine with a heat leak. For each of the four heat transfer laws the parameters of the engine are chosen in a way such that the maximum power output was equal. The heat leak for all four systems is defined

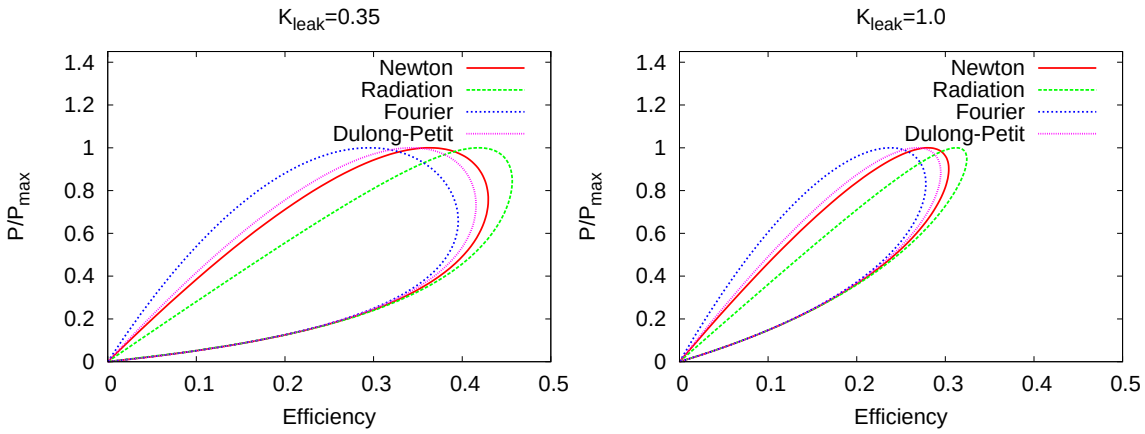

Figure 4.11: Power vs. efficiency for a Novikov engine with different heat transfer laws and a heat leak. The temperatures of the external heat baths are the same for each curve. In the plot on the left side the parameter K_{leak} is 0.35 and in the right plot it is 1.0, i.e. more heat is lost through the leak. (For the Dulong-Petit heat transfer $n = 1.25$.)

as an irreversible interaction between the two external heat baths. It is characterised by Newtonian heat transfer with the heat conductance K_{leak}:

$$q_{\text{leak}} = K_{\text{leak}}(T_{\text{H}} - T_{\text{L}}). \tag{4.40}$$

In case of heat leak the maximum efficiency depends on the heat transfer law. It is biggest for radiation and smallest for the Fourier heat transfer law.

5 Chemical engines

Another important group of endoreversible engines are chemical engines. The exchanged extensities for chemical engines, i.e. the particles, can for instance consist of electrons (e.g. in solar cells) or molecules (e.g. gas exchange in the respiratory system). Biological systems, electro-chemical, and photochemical devices are examples for chemical engines.

In this chapter a special kind of chemical engines is discussed. In the way they operate they are similar to the heat engines discussed before. In heat engines temperature differences are transformed into work while in the chemical engines presented here, work is generated because of differences in the chemical potential. Chemical potential and particle transfer are then comparable to temperature and heat transfer.

5.1 Analytical approach to a chemical engine

Chemical engines have been widely discussed and compared to Curzon-Ahlborn engines in terms of power output and performance measures [7, 11, 14]. In the following the detailed structure of a chemical engine as well as the calculation of the power output and efficiency are presented.

Figure 5.1 shows an endoreversible heat engine next to an endoreversible chemical engine. The heat engine is the Curzon-Ahlborn engine discussed in section 4.1 and the chemical engine was designed with a comparable structure. The similarities imply that the same set of endoreversible reasoning as for heat engines can be applied to chemical engines. Analogue to the transport equations for heat the particle flows are given by

$$J_{\mathrm{H}} = h_{\mathrm{H}}(\mu_{\mathrm{H}} - \mu_{\mathrm{iH}}) \quad \text{and} \tag{5.1}$$

$$J_{\mathrm{L}} = h_{\mathrm{L}}(\mu_{\mathrm{iL}} - \mu_{\mathrm{L}}), \tag{5.2}$$

where J_{H} denotes the particle flow between the high chemical potential reservoir and the engine and J_{L} denotes the particle flow between the engine and the low chemical potential reservoir. However, in the scheme of endoreversible thermodynamics heat transfer and particle transfer are not the same. While the heat transfer is a form of an energy flux, the particle transfer is a flux of an extensity. Thus the behaviour of a chemical engine is different from that of a heat engine.

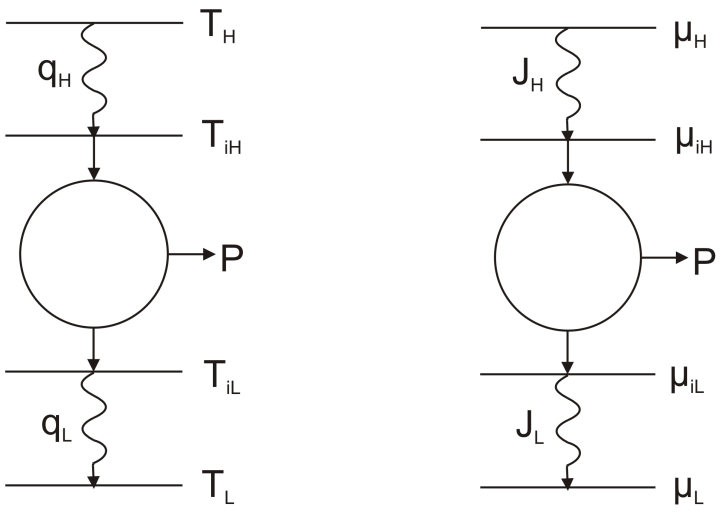

Figure 5.1: Comparison of a Curzon-Ahlborn engine on the left side and a chemical engine on the right side. Both consist of an engine, which is connected irreversible with two external infinite reservoirs.

The balance equations for such a chemical engine differ slightly from those of the Curzon-Ahlborn engine:

$$0 = \mu_{\mathrm{iH}} J_{\mathrm{H}} - \mu_{\mathrm{iL}} J_{\mathrm{L}} - P, \tag{5.3}$$

$$0 = J_{\mathrm{H}} - J_{\mathrm{L}}. \tag{5.4}$$

Equation 5.4 follows directly from the mass conservation law, i.e. the particle flows have to add up to zero. Therefore it is convenient to set $J_{\mathrm{H}} = J_{\mathrm{L}} \equiv J$.
Thus, with the help of equations 5.1 and 5.2, the power output becomes

$$P = J(\mu_{\mathrm{iH}} - \mu_{\mathrm{iL}}) = J\left(\mu_{\mathrm{H}} - \mu_{\mathrm{L}} - J\left(\frac{1}{h_{\mathrm{H}}} + \frac{1}{h_{\mathrm{L}}}\right)\right) \tag{5.5}$$

and the efficiency for such a chemical engine is given by

$$\eta = \frac{P}{\mu_{\mathrm{H}} J} = 1 - \frac{\mu_{\mathrm{L}}}{\mu_{\mathrm{H}}} - \frac{J}{\mu_{\mathrm{H}}}\left(\frac{1}{h_{\mathrm{H}}} + \frac{1}{h_{\mathrm{L}}}\right). \tag{5.6}$$

To get the point of maximum power output, the first derivative of P with respect to J is set zero:

$$\frac{\partial P}{\partial J} = \mu_{\mathrm{H}} - \mu_{\mathrm{L}} - 2J\left(\frac{1}{h_{\mathrm{H}}} + \frac{1}{h_{\mathrm{L}}}\right) = 0. \tag{5.7}$$

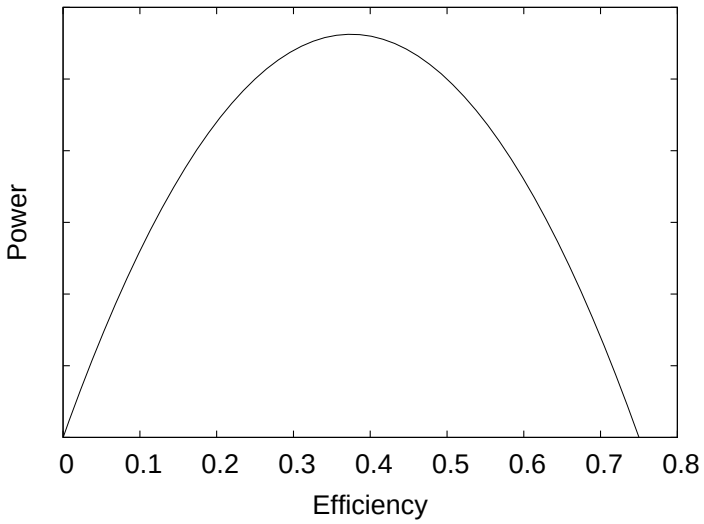

Figure 5.2: Power vs. efficiency plot for a chemical engine with the parameters $h_{\mathrm{H}} = h_{\mathrm{L}} = 1$ and the ratio $\mu_{\mathrm{L}}/\mu_{\mathrm{H}} = 1/4$. The maximum efficiency is $\eta_{\max} = 0.75$ and the efficiency at the point of maximum power output is $\eta(P_{\max}) = 0.5\eta_{\max} = 0.375$.

Thus the optimal particle flux is

$$J_{\mathrm{opt}} = (\mu_{\mathrm{H}} - \mu_{\mathrm{L}}) \frac{h_{\mathrm{H}} h_{\mathrm{L}}}{2(h_{\mathrm{H}} + h_{\mathrm{L}})}. \tag{5.8}$$

By inserting 5.8 into 5.5 the maximum power is obtained:

$$P_{\max} = (\mu_{\mathrm{H}} - \mu_{\mathrm{L}})^2 \frac{h_{\mathrm{H}} h_{\mathrm{L}}}{4(h_{\mathrm{H}} + h_{\mathrm{L}})}. \tag{5.9}$$

The efficiency at the point of optimal particle flux is

$$\eta(J_{\mathrm{opt}}) = 1 - \frac{\mu_{\mathrm{L}}}{\mu_{\mathrm{H}}} - \frac{\mu_{\mathrm{H}} - \mu_{\mathrm{L}}}{2\mu_{\mathrm{H}}} = \frac{1}{2}\left(1 - \frac{\mu_{\mathrm{L}}}{\mu_{\mathrm{H}}}\right). \tag{5.10}$$

The maximum efficiency for this system is at the point $J = 0$:

$$\eta_{\max} = 1 - \frac{\mu_{\mathrm{L}}}{\mu_{\mathrm{H}}}. \tag{5.11}$$

Thus the efficiency for the operation point with maximum power output is half of the maximum efficiency.

Also the maximum efficiency is of the same structure as the Carnot efficiency with the difference that here the ratio between the low and high temperature is exchanged for the ratio between the low and high chemical potential.

Combining equations 5.5 and 5.6 gives an equation for the power depending on the efficiency:

$$P(\eta) = \left(\frac{1}{h_\mathrm{H}} + \frac{1}{h_\mathrm{L}}\right)^{-1} \eta\mu_\mathrm{H}(\mu_\mathrm{H} - \mu_\mathrm{L} - \eta\mu_\mathrm{H}). \tag{5.12}$$

A plot of the power versus the efficiency can be seen in figure 5.2. For this curve the ratio $\mu_\mathrm{L}/\mu_\mathrm{H}$ is 1/4 and thus the maximum efficiency is $\eta_\mathrm{max} = 1 - \mu_\mathrm{L}/\mu_\mathrm{H} = 0.75$. The efficiency at maximum power is $\eta(P_\mathrm{max}) = 0.5(1 - \mu_\mathrm{L}/\mu_\mathrm{H}) = 0.375$.

5.1.1 Chemical engines in 'ETA-Graphics'

The model of a chemical engine in 'ETA-Graphics' is shown in figure 5.3. It is similar to the Curzon-Ahlborn engine except that the heat reservoirs are exchanged for particle reservoirs. The high chemical potential reservoir is denoted with 1 and the low chemical potential reservoir is denoted with 4. Interaction C is characterised by the carrier flow J_H. Interaction D is characterised by the carrier flow J_L. With the notation of 'ETA-Graphics' the particle flows become

$$J_\mathrm{H} = h_\mathrm{H}(\mu_\mathrm{1C} - \mu_\mathrm{0C}) \quad \text{and} \tag{5.13}$$

$$J_\mathrm{L} = h_\mathrm{L}(\mu_\mathrm{0D} - \mu_\mathrm{4D}), \tag{5.14}$$

where μ_1C is equivalent to μ_H, $\mu_\mathrm{0C} \equiv \mu_\mathrm{iH}$, $\mu_\mathrm{0D} \equiv \mu_\mathrm{iL}$ and $\mu_\mathrm{4D} \equiv \mu_\mathrm{L}$. Since both of these interactions are irreversible, entropy is produced. To deposit this entropy and part of the energy, additional reservoirs are included (subsystems 6 and 7 in figure 5.3).

The energy fluxes at interaction C are

$$I_\mathrm{1C} = h_\mathrm{H}(\mu_\mathrm{1C} - \mu_\mathrm{0C})\mu_\mathrm{1C} \quad \text{and} \tag{5.15}$$

$$I_\mathrm{0C} = h_\mathrm{H}(\mu_\mathrm{1C} - \mu_\mathrm{0C})\mu_\mathrm{0C} \tag{5.16}$$

at the beginning and the end of the interaction arrow respectively. For the energy at the additional subsystem 6 follows:

$$I_\mathrm{6F} = I_\mathrm{1C} - I_\mathrm{0C} = h_\mathrm{H}(\mu_\mathrm{1C} - \mu_\mathrm{0C})(\mu_\mathrm{1C} - \mu_\mathrm{0C}) = h_\mathrm{H}(\mu_\mathrm{1C} - \mu_\mathrm{0C})^2. \tag{5.17}$$

The energy fluxes at interaction D are defined in an analogous way.

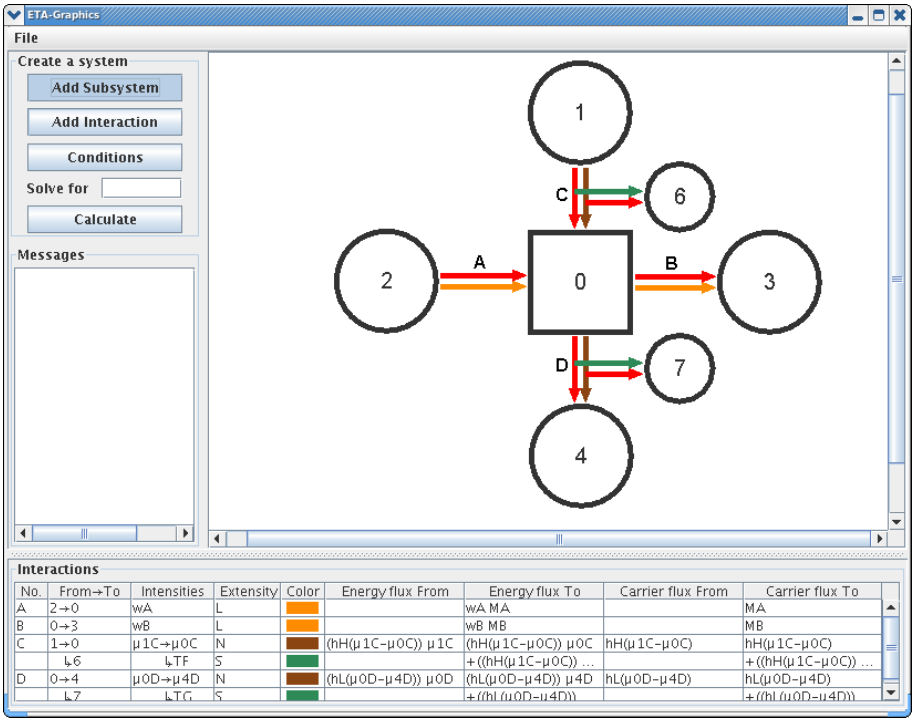

Figure 5.3: A chemical engine in 'ETA-Graphics'. Subsystem 1 and 4 are high and low chemical potential reservoirs. Subsystem 2 and 3 are reservoirs with angular velocity as the intensity and subsystems 6 and 7 are the reservoirs where the entropy, produced at the irreversible interactions C and D, is deposited.

Interactions A and B are direct contacts between the engine and the reservoirs with angular momentum L as the extensity and angular velocity ω as the corresponding intensity. In the following only the angular momentum flux, i.e. the torque M, appears.

By solving the balance equations for ω_B, M_B and $\mu_{0\mathrm{D}}$ with 'ETA-Graphics' one gets the following solutions:

$$\omega_\mathrm{B} = \frac{h_\mathrm{H}(\mu_{1\mathrm{C}} - \mu_{0\mathrm{C}})(h_\mathrm{L}(\mu_{0\mathrm{C}} - \mu_{4\mathrm{D}}) - h_\mathrm{H}(\mu_{1\mathrm{C}} - \mu_{0\mathrm{C}}))}{h_\mathrm{L} M_\mathrm{A}}, \tag{5.18}$$

$$M_\mathrm{B} = M_\mathrm{A}, \tag{5.19}$$

$$\mu_{0\mathrm{D}} = \frac{h_\mathrm{H}(\mu_{1\mathrm{C}} - \mu_{0\mathrm{C}})}{h_\mathrm{L}} + \mu_{4\mathrm{D}}. \tag{5.20}$$

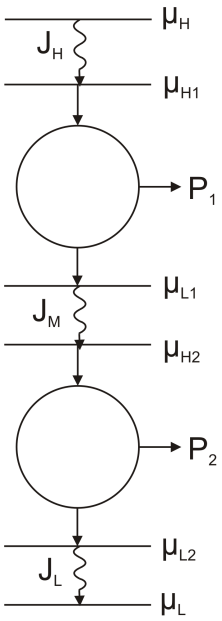

Figure 5.4: Structure of a two-staged chemical engine. The circles represent the two engines, the first one working between the chemical potentials μ_{H1} and μ_{L1} and the second one between μ_{H2} and μ_{L2}. The waved lines represent irreversible interactions and P_1 and P_2 denote the power output of the engines.

Thus the power output P becomes

$$P = \omega_{\mathrm{B}} M_{\mathrm{B}} = \frac{h_{\mathrm{H}}(\mu_{1\mathrm{C}} - \mu_{0\mathrm{C}})(h_{\mathrm{L}}(\mu_{0\mathrm{D}} - \mu_{4\mathrm{D}}) - h_{\mathrm{H}}(\mu_{1\mathrm{C}} - \mu_{0\mathrm{C}}))}{h_{\mathrm{L}}}. \tag{5.21}$$

5.2 Staged chemical engines

This section deals with two-staged chemical engines. The same chemical engines as in the section before are used but now two of them are coupled in a way such that the reservoir with the lower chemical potential of the first engine is replaced by a second engine. Thus the particle flux leaving the first engine is totally used as the particle source of the second engine. This structure is similar to that of the two-staged heat engine discussed in section 4.3.

Chen et al. [8] presented a cyclic operating two-staged chemical engine. Here the same calculations are made for a steady-state engine.

The structure of a two-staged engine can be seen in figure 5.4. It operates between a reservoir of high chemical potential μ_{H} and a reservoir of low chemical potential μ_{L}. The particle flow between the high potential reservoir and the first engine is denoted with J_{H} and is of the form

$$J_{\mathrm{H}} = h_{\mathrm{H}}(\mu_{\mathrm{H}} - \mu_{\mathrm{H1}}). \tag{5.22}$$

Analogue the particle fluxes between the two engines and between the second engine and the low chemical potential reservoir are

$$J_{\mathrm{M}} = h_{\mathrm{M}}(\mu_{\mathrm{L1}} - \mu_{\mathrm{H2}}) \quad \text{and} \tag{5.23}$$

$$J_{\mathrm{L}} = h_{\mathrm{L}}(\mu_{\mathrm{L2}} - \mu_{\mathrm{L}}). \tag{5.24}$$

Because of the conservation of mass and the restriction that no mass is transported through the power output contacts, all three particle fluxes are equal. Thus it is convenient to introduce $J \equiv J_{\mathrm{H}} = J_{\mathrm{M}} = J_{\mathrm{L}}$.

The corresponding energy fluxes are $\mu_{\mathrm{H}}J$ at the high chemical potential reservoir, $\mu_{\mathrm{H1}}J$ at the first engine's contact point with high chemical potential, $\mu_{L1}J$ at the low chemical potential contact point of the same engine and so on.

The energy balance equations for the two coupled engines are

$$P_1 = \mu_{\mathrm{H1}}J - \mu_{\mathrm{L1}}J \text{ and} \tag{5.25}$$

$$P_2 = \mu_{\mathrm{H2}}J - \mu_{\mathrm{L2}}J. \tag{5.26}$$

Thus the total power output is

$$P = P_1 + P_2 = J(\mu_{\mathrm{H1}} + \mu_{\mathrm{H2}} - \mu_{\mathrm{L1}} - \mu_{\mathrm{L2}}). \tag{5.27}$$

With equations 5.22, 5.23 and 5.24 we obtain

$$P = J\left(\mu_{\mathrm{H}} - \mu_{\mathrm{L}} - J\left(\frac{1}{h_{\mathrm{H}}} + \frac{1}{h_{\mathrm{M}}} + \frac{1}{h_{\mathrm{L}}}\right)\right). \tag{5.28}$$

Maximising with respect to J gives the optimal particle flux:

$$\frac{\partial P}{\partial J} = \left(\mu_{\mathrm{H}} - \mu_{\mathrm{L}} - 2J\left(\frac{1}{h_{\mathrm{H}}} + \frac{1}{h_{\mathrm{M}}} + \frac{1}{h_{\mathrm{L}}}\right)\right) = 0 \tag{5.29}$$

$$J_{\mathrm{opt}} = \frac{h_{\mathrm{H}}h_{\mathrm{M}}h_{\mathrm{L}}}{2(h_{\mathrm{M}}h_{\mathrm{L}} + h_{\mathrm{H}}h_{\mathrm{L}} + h_{\mathrm{H}}h_{\mathrm{M}})}(\mu_{\mathrm{H}} - \mu_{\mathrm{L}}). \tag{5.30}$$

By inserting the result from 5.30 into the power equation 5.28 one gets

$$P_{\max} = (\mu_{\mathrm{H}} - \mu_{\mathrm{L}})^2 \frac{h_{\mathrm{H}}h_{\mathrm{M}}h_{\mathrm{L}}}{4(h_{\mathrm{M}}h_{\mathrm{L}} + h_{\mathrm{H}}h_{\mathrm{L}} + h_{\mathrm{H}}h_{\mathrm{M}})}. \tag{5.31}$$

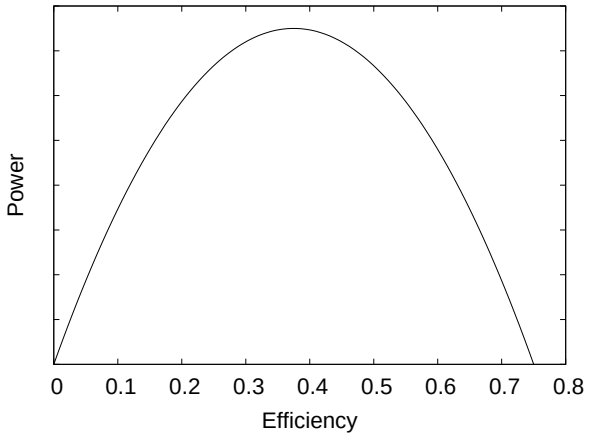

Figure 5.5: Power-efficiency plot for a two-staged chemical engine with $\mu_{\mathrm{L}}/\mu_{\mathrm{H}} = 1/4$. For the point of maximum power output the efficiency is $\eta(P_{\max}) = 0.5(1-\mu_{\mathrm{L}}/\mu_{\mathrm{H}}) = 0.38$ and the maximum efficiency is $\eta_{\max} = 1-\mu_{\mathrm{L}}/\mu_{\mathrm{H}} = 0.75$.

The efficiency for this system can be written as the ratio of the mechanical power output and the chemical energy influx:

$$\eta = \frac{P}{\mu_{\mathrm{H}} J} = 1 - \frac{\mu_{\mathrm{L}}}{\mu_{\mathrm{H}}} - \frac{J}{\mu_{\mathrm{H}}} \left(\frac{1}{h_{\mathrm{H}}} + \frac{1}{h_{\mathrm{M}}} + \frac{1}{h_{\mathrm{L}}} \right) \tag{5.32}$$

and thus the efficiency at the point of maximum power output is

$$\eta(J_{\mathrm{opt}}) = 1 - \frac{\mu_{\mathrm{L}}}{\mu_{\mathrm{H}}} - \frac{\mu_{\mathrm{H}} - \mu_{\mathrm{L}}}{2\mu_{\mathrm{H}}} = \frac{1}{2} \left(1 - \frac{\mu_{\mathrm{L}}}{\mu_{\mathrm{H}}} \right). \tag{5.33}$$

This result, which is the same as for the single chemical engine described in section 5.1, shows that the efficiency at the point of maximum power output does not depend on the staging of the engines but only on the ratio of the outer chemical potentials between which the engine is working.

Also the maximum efficiency for the staged engine is

$$\eta_{\max} = 1 - \frac{\mu_{\mathrm{L}}}{\mu_{\mathrm{H}}} \tag{5.34}$$

like for the single chemical engine described before.

An equation for the power depending on the efficiency can be obtained by combining equations 5.28 and 5.32:

$$P(\eta) = \left(\frac{1}{h_\mathrm{H}} + \frac{1}{h_\mathrm{M}} + \frac{1}{h_\mathrm{L}}\right)^{-1} \eta\mu_\mathrm{H}(\mu_\mathrm{H} - \mu_\mathrm{L} - \eta\mu_\mathrm{H}). \tag{5.35}$$

A curve of the power over the efficiency can be seen in figure 5.5. It has the same shape as for a single chemical engine with the only difference that the power output of the staged chemical engine is lower than that of the single engine if the coefficients h_i are all equal (i.e. $h_\mathrm{H} = h_\mathrm{M} = h_\mathrm{L}$). Comparing equations 5.12 and 5.35 gives the scaling factor between the power for a single chemical engine and the power of two connected chemical engines:

$$P_\mathrm{staged} = \frac{\frac{1}{h_\mathrm{H}} + \frac{1}{h_\mathrm{L}}}{\frac{1}{h_\mathrm{H}} + \frac{1}{h_\mathrm{M}} + \frac{1}{h_\mathrm{L}}} P_\mathrm{single}. \tag{5.36}$$

Thus the power output of a two-staged engine is 2/3 of the power output of a single engine for $h_\mathrm{H} = h_\mathrm{M} = h_\mathrm{L}$.

5.2.1 Staged chemical engines in 'ETA-Graphics'

Figure 5.6 shows the structure of a two-staged chemical engine in 'ETA-Graphics'. Subsystem 1 represents the high chemical potential reservoir and subsystem 8 represents the low chemical potential reservoir. Subsystems 0 and 5 are the two chemical engines. The interactions C, E, and H are characterised by the particle flows according to equations 5.22 to 5.24. These interactions are irreversible and the produced entropy cannot be deposited via the two contact points of this interaction. Thus for each of these interactions an additional subsystem is added (subsystems 9 to 11). Interactions A, B, F, and G represent direct contacts between the engines and the reservoirs with angular momentum as their extensity and angular velocity as the corresponding intensity.

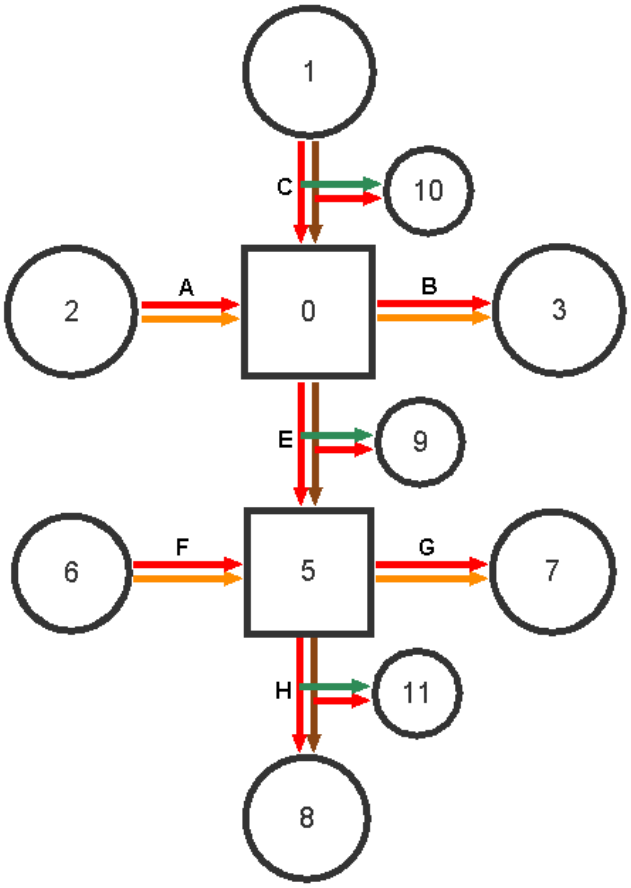

Figure 5.6: A two-staged chemical engine in 'ETA-Graphics'. Subsystems 0 and 5 are the two chemical engines. Subsystem 1 is the high chemical potential reservoir and subsystem 8 is the low chemical potential reservoir.

6 Conclusion

In this work I presented 'ETA-Graphics', an interface to endoreversible thermodynamics. Its structure and functions were presented and analytical results for some heat and chemical engines were compared with the results produced by the application. The application is capable of doing evaluations for steady state or cyclic engines and infinite reservoirs. The efficiency as well as the total power output of an engine can be calculated and plotted against each other. So far it is not possible to include finite reservoirs into systems created with 'ETA-Graphics'. Since finite reservoirs would cause differential equations, they would lead to much more complicated calculations.
Sometimes the automatic choice of variables for which the equation system should be solved is not good enough. Especially for staged systems it happens that the equation system cannot be solved for the chosen variables but this can be easily fixed. The user just has to choose the variables himself or at least change some of the proposed ones.

Curzon-Ahlborn and Novikov-like heat engines in different constellations have been investigated in great detail with 'ETA-Graphics' (section 2.2 and chapter 4). For example Rubin and Andresen [21] showed, that the efficiency of an endoreversible Curzon-Ahlborn heat engine does not change when the single engine is replaced by two combined Curzon-Ahlborn engines working between the same temperatures. In the system with the staged heat engines the waste heat of the first engine is totally used as the heat source of the second engine. The power output, however, decreases because of the higher heat resistance of the system. These results have been reproduced with the help of 'ETA-Graphics'.
The influence of a heat leak, formerly described in [4, 13], has been discussed as well as the influence of different heat transfer laws. The heat leak causes a closed loop in the power-efficiency plot and the efficiency at maximum power output as well as the maximum efficiency decrease with increasing amount of heat lost through the leak.
Different heat transfer laws, like Radiation, Newtonian, and Fourier heat transfer, influence the shape of the power-efficiency curve. The efficiencies at maximum power output differ while the maximum efficiency stays constant for the same external bath temperatures.

The second group of engines, which have been discussed in this work, are chemical engines. They are similar to Curzon-Ahlborn engines in their structure but they also

show some not negligible differences. The heat transfer laws for heat engines have the same structure as the particle transfer laws for the chemical engines. However, in the picture of endoreversible thermodynamics the particle transfer is an extensity flow while the heat transfer is an energy flow. Thus the balance equations for the engines are slightly different, which leads, for instance, to different power-efficiency curves.

Bibliography

[1] F. Angulo-Brown and R. Páez-Hernández. Endoreversible Thermal Cycle with a Nonlinear Heat Transfer Law. *J. Appl. Phys.*, 74(4):2216–2219, 1993.

[2] A. Bejan. *Advanced Engineering Thermodynamics*. John Wiley & Sons, New York, 1988.

[3] Sadi Carnot. *Réflexions sur la puissance motrice du feu et sur les machines propres á développer cette puissance*. Bachelier, Paris, 1824. in French, Bachelier, Paris, 1824; Fox, R. (ed.), Libraire Philosophique J. Vrin, Paris 1978, see also On the Motive Power of Heat, American Society of Mechanical Engineers, 1943).

[4] Jincan Chen. The Maximum Power Output and Maximum Efficiency of an Irreversible Carnot Heat Engine. *J. Phys. D: Appl. Phys.*, 27:1144–1149, 1994.

[5] Jincan Chen. Thermodynamic and thermoeconomic analysis of an irreversible combined Carnot heat engine system. *Int. J. Energy Res.*, 25:413–426, 2001.

[6] Jincan Chen and Chih Wu. Maximum Specific Power Output of a Two-Stage Endoreversible Combined Cycle. *Energy*, 20(4):305–309, 1995.

[7] L. G. Chen, F. R. Sun, C. Wu, and J. Yu. Performance characteristic of isothermal chemical engines. *Energy Conversion and Management*, 38(18):1841–1846, 1997.

[8] L. G. Chen, F. R. Sun, C. H. Wu, and J. Z. Gong. Maximum power of a combined-cycle isothermal chemical engine. *Appl. Thermal Eng.*, 17(7):629–637, 1997.

[9] F. L. Curzon and B. Ahlborn. Efficiency of a Carnot Engine at Maximum Power Output. *Am. J. Phys.*, 43:22–24, 1975.

[10] Alexis De Vos. Efficiency of some Heat Engines at Maximum-Power Conditions. *Am. J. Phys.*, 53:570–573, 1985.

[11] Alexis De Vos. Endoreversible Thermodynamics and Chemical Reactions. *J. Phys. Chem.*, 95:4534–4540, 1991.

[12] J. M. Gordon. Observations on Efficiency of Heat Engines Operating at Maximum Power. *Am. J. Phys.*, 58(4):370–375, 1990.

[13] J. M. Gordon and Mahmoud Huleihil. General Performance Characteristics of Real Heat Engines. *J. Appl. Phys.*, 72(3):829–837, 1992.

[14] J. M. Gordon and V. N. Orlov. Performance Characteristics of Endoreversible Chemical Engines. *J. Appl. Phys.*, 74(9):5303–5309, 1993.

[15] K. H. Hoffmann. An introduction to endoreversible thermodynamics. *Atti dell Accademia Peloritana dei Pericolanti - Classe di Scienze Fisiche, Matematiche e Naturali*, pages 1–19, 2007.

[16] K. H. Hoffmann, J. Burzler, A. Fischer, M. Schaller, and S. Schubert. Optimal Process Paths for Endoreversible Systems. *J. Non-Equilib. Thermodyn.*, 28(3):233–268, 2003.

[17] K. H. Hoffmann, J. M. Burzler, and S. Schubert. Endoreversible Thermodynamics. *J. Non-Equilib. Thermodyn.*, 22(4):311–355, 1997.

[18] I. I. Novikov. The Efficiency of Atomic Power Stations. *Journal Nuclear Energy II*, 7:125–128, 1958. translated from Atomnaya Energiya, 3 (1957), 409.

[19] Morton H. Rubin. Optimal Configuration of a Class of Irreversible Heat Engines. I. *Phys. Rev. A*, 19(3):1272–1276, 1979.

[20] Morton H. Rubin. Optimal Configuration of a Class of Irreversible Heat Engines. II. *Phys. Rev. A*, 19(3):1277–1289, 1979.

[21] Morton H. Rubin and Bjarne Andresen. Optimal Staging of Endoreversible Heat Engines. *J. Appl. Phys.*, 53(1):1–7, 1982.

[22] Wolfram Research, Inc. *Mathematica, Version 6.0.0.* Champaign, Illinois, 2007.

Selbständigkeitserklärung

Hiermit erkläre ich, dass ich die vorliegende Arbeit selbständig angefertigt, nicht anderweitig zu Prüfungszwecken vorgelegt und keine anderen als die angegebenen Hilfsmittel verwendet habe. Sämtliche wissentlich verwendete Textausschnitte, Zitate oder Inhalte anderer Verfasser wurden ausdrücklich als solche gekennzeichnet.

Chemnitz, den 07. Juli 2008

Katharina Wagner